Contents list available at IJRED website

International Journal of Renewable Energy Development

Journal homepage: https://ijred.undip.ac.id

Review Article

Transition metal-based materials and their catalytic influence on MgH_2 hydrogen storage: A review

Oluwashina Philips Gbenebor* and Abimbola Patricia Idowu Popoola

Department of Chemical, Metallurgical and Materials Engineering, Tshwane University of Technology, Pretoria, South Africa

Abstract. The dependence on fossil fuels for energy has culminated in its gradual depletion and this has generated the need to seek alternative source that will be environmentally friendly and sustainable. Hydrogen stands to be promising in this regard as energy carrier which has been proven to be efficient. Magnesium hydride (MgH_2) can be used in storing hydrogen because of its availability, light weight and low cost. In this review, monoatomic, alloy, intermetallic and composite forms of Ti, Ni, V, Mo, Fe, Cr, Co, Zr and Nb as additives on MgH_2 are discussed. Through ball milling, additive reacts with MgH_2 to form compounds including TiH_2, Mg_2Ni, Mg_2NiH_4, V_2O, VH_2, MoSe, Mg_2FeH_6, NbH and Nb_2O_5which remain stable after certain de/hydrogenation cycles. Some monoatomic transition metals remain unreacted even after de/hydrogenation cycles. These formed compounds, including stable monoatomic transition metals, impart their catalytic effects by creating diffusion channels for hydrogen via weakening Mg - H bond strength. This reduces hydrogen de/sorption temperatures, activation energies and in turn, hastens hydrogen desorption kinetics of MgH_2. Hydrogen storage output of MgH_2/transition metal-based materials depend on additive type, ratio of MgH_2/additive, ball milling time, ball –to combining materials ratio and de/hydrogenation cycle. There is a need for more investigations to be carried out on nanostructured binary and ternary transition metal-based materials as additives to enhance the hydrogen storage performance of MgH_2. In addition, the already established compounds (listed above) formed after ball milling or dehydrogenation can be processed and directly doped into MgH_2.

Keywords: Dehydrogenation; Fossil fuel; Hydride; Hydrogenation; Transition metal

Received: 30th August 2023; Revised: 8th Oct 2023; Accepted: 26st Oct 2023; Available online: 31st Oct 2023

Introduction

Rapid growth in human productive engagements (aimed at improving standards of living) over the years have brought about urbanization. This has led to drastic population growth and placed a huge stress on energy generation and its utilization globally. The world community at large has been plagued with consequences of global warming owing to its large dependence on fossil fuels since the emergence of industrial revolution. These non-renewable resources have largely played a dominant role in energy production, maintenance and transportation. It has been reported by the United States Environmental Protection Agency (US EPA) that carbon dioxide (CO_2) maintains the highest constituent (Figure 1a) among the greenhouse gases (US EPA, 2023). This gas is often released during burning of fossil fuels such as oil, coal, natural gas (Stephen, 2005), deforestation (Van der Werf *et al.* 2009) and other industrial/manufacturing activities (Figure 1b). It causes global warming and other health issues through hypercapnia (Yu *et al.* 2013; Shigemura et al. 2017; Taghizadeh-hesary *et al.* 2021). The basic source of energy generation for instance, as reported by Singh *et al.* (2021) entails the combustion of fossil fuels which yields the release of CO_2 before (pre-combustion) or after (post-combustion) to the atmosphere. Globally, economic growth has been seen as a catalyst for greenhouse gas existence and its emission is mostly prevalent in China (Yang *et al.* 2020). African countries largely depend on fossil fuels for energy storage and use. In a model developed by Olubusoye and Musa, (2020), it was predicted that gradual economic growth rise in African countries will engender more greenhouse gas emissions. In South Africa for instance, Oladunni *et al.* (2022) reported that economic and population growths are the two major elements that have triggered the emission of greenhouse gas, most especially in the transport sector.

Efforts therefore are being made to produce renewable and sustainable energy that is friendly to the ecosystem. Hydrogen energy stands out as a renewable secondary energy which is clean, sustainable and can be used as an energy carrier and fuel cells. It is not like gas, coal or oil that serves as a primary energy source; hydrogen needs to be produced from another energy source (preferably from renewable sources in this case) such as biomass, wind, solar, hydro and geothermal. As the most abundant element in the universe, hydrogen is affirmed to be the ideal energy source in the 21st century that can be synthesized via water electrolysis with no pollutant released (Hou *et al.* 2021).

2. Hydrogen storage

Hydrogen is often stored as compressed gas, cryogenic liquid or in solid state. Liquid hydrogen is used as fuel for low temperature rockets and mobile applications (Al Ghafr *et al.*

* Corresponding author
Email: philipsogbenebor@gmail.com (O.P.Gbenebor)

https://doi.org/10.14710/ijred2023.57805
ISSN: 2252-4940/© 2023.The Author(s). Published by CBIORE

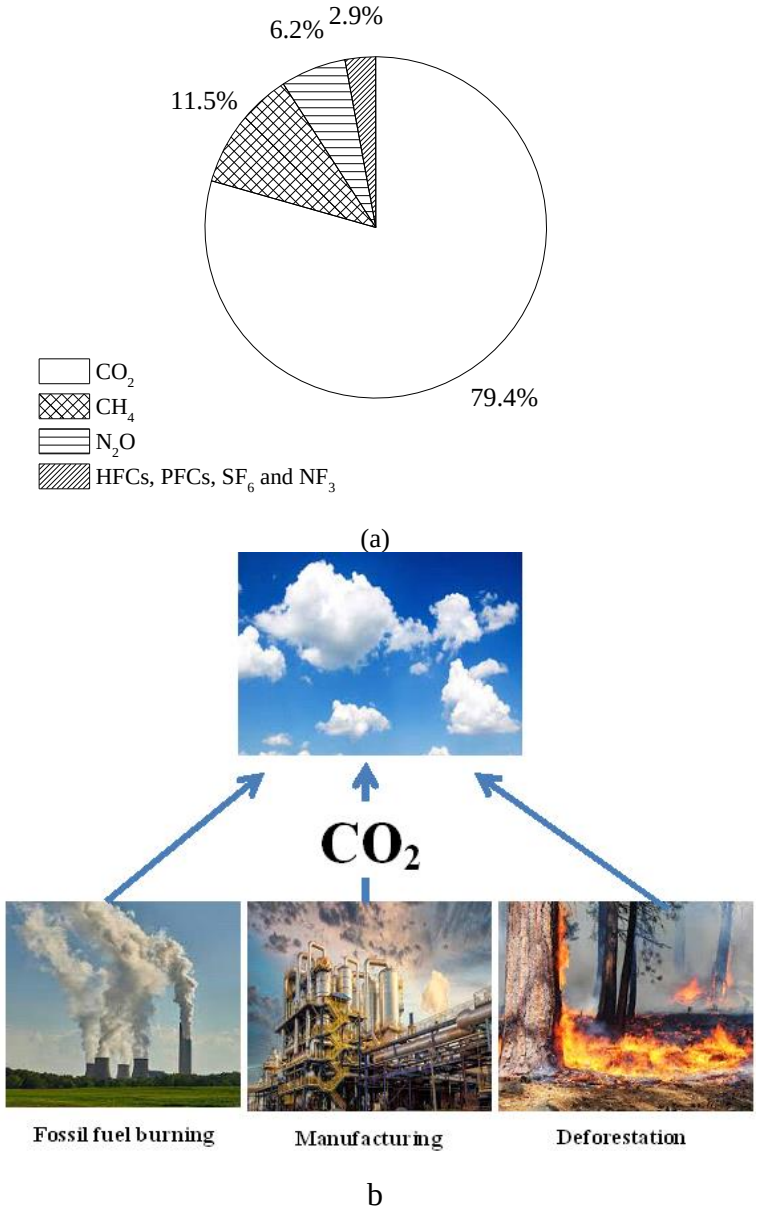

Fig 1.(a) Percentage constituents of greenhouse gas (US EPA, 2023) (b) Major activities that result to CO_2 emission**.**

2022; Jiang *et al.* 2023). It has been reported that cryogenic liquid hydrogen can be stored at -253 °C and 1 bar (Krishna *et al.* 2012); at this temperature, it maintains a density approximately 71 gL^{-1} (Edwards, *et al.* 2007). In the sphere of energy and space missions, the main tools to consider in liquid hydrogen storage are materials for transportation vessels and cryogenic storage. Alloys of titanium (Madina & Azkarate, 2009), steel (Krainz, *et al.* 2004) and aluminum-lined composites (Aceves *et al.* 2000; Aceves *et al.* 2010) have been used for the storage and transportation of cryogenic liquid hydrogen but drawbacks have been witnessed in their impact strength, ductility and toughness at low temperatures. Design and development of highly effective low temperature materials for cryogenic liquid hydrogen storage is being advocated for (Qiu et al. 2021). A methodical insulation needs to be devised in other to maintain hydrogen in its liquid phase because of its low boiling point in this cryogenic state. Storage in the compressed gaseous form is another common method to store hydrogen. Materials such as steel (Zhang *et al.* 2008) and aluminum-carbon fiber composites (Takeichi *et al.* 2003) have been used in designing vessels that can store and transport hydrogen compressed at high pressure. Unlike the liquid storage, compressed gas can be stored at room temperature (Zheng *et al.* 2012)**.** The density of hydrogen stored in the compressed gaseous state is lower compared to that of cryogenic liquid; a lower energy per unit volume has also been affirmed to be witnessed in pressurized gas (Zhang *et al.* 2016). Although both storage methods allow easy accessibility of hydrogen, there are draw backs that have bedeviled its storage and transportation. Cryogenic liquid hydrogen for instance, can only be stored for a short period to avoid the risk of steady boiling (Prabhukhot *et al.* 2016; Edalati *et al.* 2018). The low specific gravity of hydrogen creates an issue for its storage in compressed form as it requires huge magnitude of energy to achieve this, though much energy is needed for the storage of hydrogen in the liquid form compared to when compressed in gaseous state (Krishna, *et al.* 2012). In the solid state form, hydrogen molecules combine with other materials; a little volume of material can store large

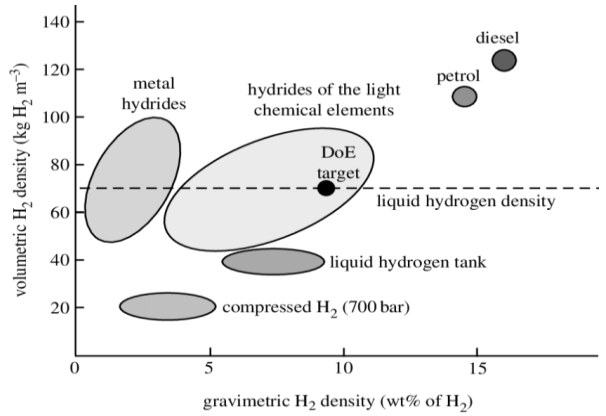

Fig. 2. Hydrogen storage methods with their volumetric and gravimetric densities (Edwards et al. 2007)

hydrogen content than the two methods earlier discussed. A solid state hydrogen storage material easily adsorbs/absorbs and desorbs hydrogen at temperatures close or equal to room temperature. Storing hydrogen in the solid-state addresses issues of safety; boil off loss, heavy vessel weights and liquefaction energy associated with pressurized and liquid hydrogen storage. The volumetric and gravimetric densities of hydrogen storage methods are presented in Figure 2.

Hydrogen can physically or chemically combine with a solid material and when needed, it is made to desorb or dissociate from the material on involvement of thermal energy or any other means such as hydrolysis as discussed by Hou *et al.* (2021). In the physical process (physisorption), molecules of hydrogen adsorb on the material surface while a chemical bond is formed when hydrogen molecules chemically react with the material (also called chemisorption as material absorbs hydrogen molecules in this case). When hydrogen adsorbs on a material, there often exists weak van der Waals interactions between its molecules and the surface of the storage material. This implies that an appropriate material surface area will be required to achieve a remarkable hydrogen storage capacity. It is being reported that low activation energy is required to execute adsorption and desorption of hydrogen molecules in this case and this is responsible for fast ad/desorption kinetics (Prabhukhot *et al.* 2016). Materials with porous structures including activated carbon, grapheme, carbon nanotubes (CNTs), porous aromatic frame works (PAFs), metal organic frame works (MOFs) and zeolites have been used (see Table 1).

A chemical bond is formed when a material absorbs hydrogen molecules into its structure. Many metals fall into this category as they reversibly react with hydrogen to form hydrides which serve as a hydrogen storage material. The ease of hydride formation and dissociation is different among metal hydrides based on the strength of bond formed between the metal and hydrogen. For a metal hydride to be classified as suitable for hydrogen storage for energy use, it needs to possess High volumetric and gravimetric densities. Fast hydrogen release (during dissociation) at a reduced temperature and adequate pressure is also a key feature required of a metal hydride as this saves time and energy. Aluminum hydride (AlH_3) for example, is affirmed to decompose into its constituent elements rapidly at room temperature and 700 bar with enthalpy of formation ranging between -6 to 7.6 kJ/mol (Zidan, 2010). This implies that it has fast dehydrogenation kinetics which qualifies it as a good storage material. Jieng *et al.* (2021) highlighted the high pressure (700 bar) as an issue when considering hydrogen storage on a large scale. Another class of hydride called complex hydride contains a counter ion with a coordination complex where hydrogen is covalently bonded. Electropositive Li^+ for instance, reacts with $(BH)^-$ to form $Li(BH_4)$. Prabhukhot *et al.* (2016) gave the complex hydride representation as $A_xMe_yH_z$ where elements in the first and second groups in the periodic table fit into "A" while "Me" is often occupied by aluminum or boron. Some other complex

Table1
Hydrogen adsorption capacities of some activated carbon, metal organic frame works, porous aromatic frame works and zeolites

	H_2 storage caapcity (%)	ref.
Activated carbon	7.88% 2 bar 77 K	(Wang *et al.* 2009)
	4.6%% 10 bar , 77 K	(Chen *et al.* 2008)
	2.96% at 1 bar and 77 K	(Sethia & Sayar, 2016)
	2.85% at 1 bar and 77 K	(Wrobel-Iwaniec *et al.* 2015)
	2.50% at 1bar and 77 K	(Liu *et al.* 2014)
	0.2% 30 bar and room temp.	(Doğan *et al.* 2020)
Carbon nanotubes	19% at 100 bar and 77 K	(Assfour *et al.* 2011)
	5.5% at 100 bar and 300 K	(Assfour *et al.* 2011)
	14.1%% at 70 bar and 77 K	(Farha *et al.* 2010)
Graphene	2.7% at room temp. And 25 bar	(Yuan *et al.* 2011)
	1.47% at I bar and 77 K	(Huang *et al.* 2017)
Zeolite	2.07% at 0.016 bar and 77	(Dong *et al.* 2007)
	8.33% at 20 bar and 77 K	(Dong *et al.* 2007)
	2.6% at 1 bar and 77 K	(Yang *et al.* 2007)
	0.07% at 0.1 bar and 303 K	(Nishihara *et al.* 2009)
	2.2% at 0.3 bar and 303 K	(Nishihara *et al.* 2009)
	2.19% at 15 bar and 77 K	(Langmi *et al.* 2005)
Porous aromatic frame works	6.% at 50 bar and 77 K	(Lan *et al.* 2010)
	3% at 50 bar and 150 K	(Lan *et al.* 2010)
	2.09% at 1 bar and 77 K	(Ben *et al.* 2011)
	2.7% at 1.2 bar and 77 K	(Konstas *et al.* 2012)
Metal organic frame works	17.8% at 80 bar and 77 K	(Furukawa *et al.* 2010)
	4.5% at 20 bar and 77 K	(Nathaniel *et al.* 2003)
	4.0% at 20 bar and room temp.	(Nathaniel *et al.* 2003)
	1% at 0.8 bar and room temp.	(Rosi, *et al.* 2003)
	4.5% at 0.8 bar and 77bK	(Rosi, *et al.* 2003)
	10% at 56 bar and 77 K	(Hirscher & Panella 2007)

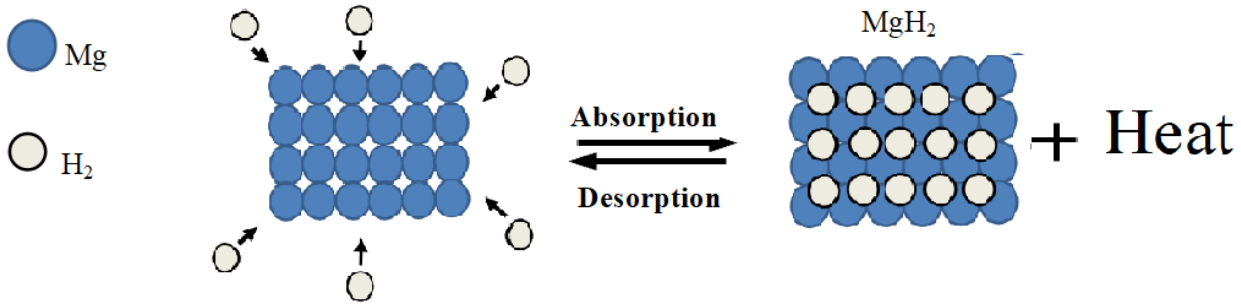

Fig 3. Schematic illustration of absorption and desorption of MgH_2

hydrides that have been synthesized include $NaAlH_4$ (Ismail *et al.* 2011; Ismail *et al.* 2012; Ud-Din *et al.* 2014), $LiAlH_4$ (Zhang *et al.* 2008; Chen *et al.* 2010) $LiNH_2$ (Luo, 2004; Chen *et al.* 2006; Barison, *et al.* 2008) and $Ca(BH_4)_2$ (Muthukumar *et al.* 2005). These materials are affirmed to be safe to handle and do not decompose easily to their stable constituents as witnessed for some metal hydrides. Complex hydrides also possess high hydrogen storage capacity. In summary, choice of hydride for solid hydrogen storage is dependent on many factors such as availability, ease of processing, cyclic stability, hydrogen storage capacity, low cost of production, dehydrogenation and hydrogenation kinetics.

Magnesium hydride (MgH_2) has been used as a storage material for hydrogen owing to its availability, light weight, huge storage capacity (7.6 wt.%), low cost of processing, good reversibility and high volumetric capacity (109 g H_2/L) (Shahi *et al.* 2015; hongtan *et al.* 2018). Low sorption kinetics has been recorded to be an issue with this material; Reaction of Mg with hydrogen to form MgH_2 (absorption) is exothermic and occurs between 250-370 ^{0}C (Figure 3); heat therefore needs to be supplied to the system for hydrogen desorption to occur.

To improve the hydrogen storage properties of the hydride, composites comprising combination of MgH_2 with one or more of carbonaceous materials (Ródena *et al.* 2008), intermetallics (Lu *et al.* 2018) oxides and hydrides of metals (including complex hydrides) have been used as catalysts.

3. Alloys compounds and composites of transition metals as catalysts

Numerous transition metals in their single forms, compounds and alloys have been used as catalysts to improve the hydrogen storage properties of MgH_2. Researches have also entailed doping MgH_2 with other non-metallic materials such as grapheme, activated carbon, carbon nanotubes and metal organic frameworks to form composites. In this section, researches on the use of transition metals in the single or monometallic forms, alloys (binary, tertiary and multicomponent) and composites with non- metallic materials as catalysts are reviewed.

3.1. Titanium (Ti)

Having established that dehydrogenation of MgH_2 will occur between 300 - 350 ^{o}C (Jin *et al.* 2007a; Croston *et al.* 2010; Li *et al.* 2013), it is expected that MgH_2-based composites should release hydrogen at a lower temperature and the activation energy required for this should reduce. Additives used impart their catalytic effects by remaining stable (unreacted) or form a new stable phase (owing to a chemical reaction) when exposed to de/hydrogenation temperatures. This boosts the hydrogen storage potency of MgH_2. Lu *et al.* (2009) employed an ultra–energy- high pressure reactive milling on MgH_2 and TiH_2 powders for 4 h at room temperature. Nanostructured combination of MgH_2 and TiH_2 were maintained after milling as no additional phase was formed. Composites remained stable after 80 cycles of dehydrogenation and hydrogenation at 300 ^{o}C. Existence of TiH_2 phase uniformly distributed in MgH_2/TiH_2 nanocomposite was reported to cause reduction in hydrogenation and dehydrogenation enthalpies. This was an additional claim to justify that asides grain size reduction, existence of well distributed stable additives will improve hydrogen storage performance of MgH_2. Twenty hours continuous milling however, culminated in the transformation of Mg and Ti to MgH_2 and TiH_2 when Shao *et al.* (2011) doped 0.1 wt.% Ti into MgH_2. Dehydrogenation of MgH_2/TiH_2 as determined by TGA/DTG curves was faster than as-milled MgH_2; the former occurred at 342 ^{o}C which was 100 ^{o}C lower than the latter (as-milled MgH_2). Unlike findings of Shao *et al,* (2011), Dehouch *et al.* (2003) earlier reported that Mg, MgO, Ti, V and Fe_2O_3 phases were formed after MgH_2 was ball milled with Ti and V. Although the milling time and temperature were not stated, it could be deduced here that the milling process engendered the dissociation of Mg from H atoms which later got oxidized to MgO on reacting with oxygen in the air. Milling condition was also sufficient to yield the formation of Fe_2O_3, which was notified as an impurity that arose from the oxidation of the steel mill balls; Ti and V remained unreacted. On cycling (de/hydrogenation cycles) at 300 ^{o}C in the presence of hydrogen-containing moisture after milling, there was an increase in hydrogen storage capacity and absorption kinetics between 500 and 1000 cycles for the composite; after the 1000th cycle, an additional phase $Mg(OH)_2$, was formed. The moisture acting as a contaminant in the hydrogen was affirmed to have engendered structural relaxation in the composite which led to its improved absorption kinetics. On the other hand, the structural modification retarded the hydrogen desorption kinetics after cycling. The investigators attributed this low kinetics to modifications that occurred on the surface of the composites. Although information regarding the mechanism involved in this surface modification was not detailed, one may suppose that $Mg(OH)_2$ and Fe_2O_3 may have a role to play in this. To further elucidate on the Findings of Lu *et al.* (2009), Hao & Scholl, (2012) deduced the mechanism responsible for the reduction in MgH_2/TiH_2 composite's enthalpy of reaction compared to single MgH_2 by adopting the first principles density functional calculations. This was used to distinguish the interfaces that could exist between MgH_2 or Mg and TiH_2. Calculations explained that strong equiaxial surfaces could exist between the low surface energy faces of MgH_2 (or Mg) and TiH_2. These interfaces induced strain on MgH_2 and Mg which was identified to be responsible for the low dehydrogenation enthalpy. Addition of 0.05, 0.1, 0.25 and 0.5 wt.% Ti, to MgH_2 and milling for 2 h have produced Mg, MgH_2 and Ti phases

(Pukazhselvan *et al*. 2020). Magnesium hydride, Ti and TiH_{2-x} (nonstoichiometric hydride) were identified when MgH_2 /0.25 wt.% Ti composite was milled for 15 h. When composites were dehydrogenated at 315 °C and 5 bars H_2 pressure after 1, 5 and 10 cycles, Ti/TiH_{2-x} was further hydrogenated to TiH_2.Titanium additive remained unreacted under 2 h (mild milling condition as defined by the researchers) milling; it was partially hydrogenated when the milling was severe (15 h) and got completed after de/hydrogenation cycles. For the strong milled composite, XPS (X-ray Photoelectron Spectroscopy) indicated that Ti existed in mixed valence states (Ti^0, Ti^{2+}, Ti^{3+}, Ti^{4+}). It was believed that Ti^{4+} (oxidation state of Ti in TiO_2) present in both samples (mild and strong miling) may have occurred as a result of surface oxidation on exposure to air. It was thus concluded that catalytic influence of Ti/TiH_2 would only be effective if MgH_2 would be milled long enough. Formation of TiH_2 during strong milling reduced the dehydrogenation activation energy of MgH_2 to 89.4 kJ/mol from 153 kJ/mol displayed by as-received MgH_2. This further justified the findings of Hao & Scholl, (2012), who suggested that when there is an equiaxial contact between Mg/MgH_2 and TiH_2, the latter would induce strain on Mg/MgH_2 contact surface which would end up lowering its dehydrogenation enthalpy. It has also been reported by Patelli *et al.* (2017) and Bhatnagar *et al.* (2018) where TiH_2 was confirmed to improve the sorption kinetics of MgH_2 by lowering the activation energy. This was also attributed to the imposition of lattice strain on MgH_2 by TiH_2. Malahayati *et al.* (2021) observed that 1 h ball milling may not be sufficient enough to induce reaction between MgH_2 and Ti powders as no change of phase was noticed after the process. Agglomerations of combining powders with increased diameter only existed during this time. After 12 h of milling, both MgH_2 and Ti still existed but this time, in nanosized form, which was attributed to the effect of energy induced by the milling process. The Ti phase disappeared after milling for 18 h while broad peaks of MgH_2 remained. It was not mentioned in the report what happened to Ti but it could be assumed that Ti was oxidized to TiH_2 which may have also led to the broadening of MgH_2 peaks that was initially narrow. The composite (MgH_2/Ti) absorbed hydrogen at 300 °C and 10 bar while desorption happened at 350 °C and 50 mbar. Both processes took place within 7 min and from previous findings of researchers, it can be deduced that TiH_2 may be responsible for the much fast kinetics compared to additive –free MgH_2. These temperatures however were outlined by the authors to be high for application purpose. Berezovets *et al.* (2022) observed that TiH_4 phase was formed using Ti nanopowder additive which led to the increase in hydrogen storage capacity of MgH_2 (6.7 wt.% H_2) (Figure 4). Milling Mg and TiO_2 nanopowders after 5 h, TiO_2 remained unreacted and this led to a low storage capacity of 5.7 wt.% H_2; it may be assumed here that the milling time was insufficient for TiO_2 to get reduced. As illustrated in Figure 4, both additives facilitated hydrogenation compared to pure Mg which implied that they aided the crystallization of MgH_2. More improved hydrogenation was realized on milling Mg powder with a suboxide of $Ti_4Fe_2O_x$ (x= 0.3, 0.5) in the presence of hydrogen pressure. The suboxide additives promoted hydrogen dissociation and the $Ti4Fe_2O_xH_y$ phase formed after milling was responsible for its highest hydrogen storage capacity (6.76 wt.% H_2). Presence of Ti, Fe and O in the suboxide created diffusion pathways for hydrogen to or from Mg/MgH_2 system during de/hydrogenation,

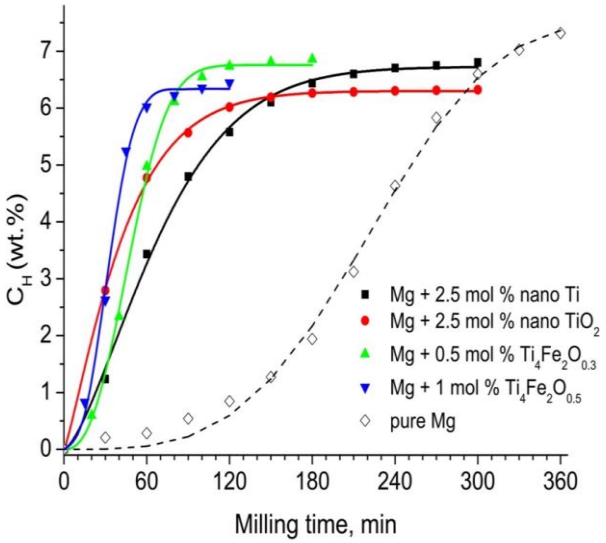

Fig 4. Hydrogen absorption capacities of Mg/Ti-based composites as a function of ball milling time (Berezovets *et al.* 2022)

Titania (TiO_2) has also been proven to be a good additive for MgH_2. Titania. MgH_2 and rock salt (Ti dissolved MgO) were reportedly formed when MgH_2 was milled with 10 wt.% TiO_2 for 5 h (Pukazhselvan *et al*. 2017a). A reduced phase, Ti_2O_3 was yielded when TiO_2 was milled with 10 wt.% MgH_2 for 30 h. A single phase rock salt was formed when MgH_2 was milled with TiO_2 in ratio 2:1. The Ti/Mg/O phase in the rock salt was confirmed to make the additive impact of TiO_2 effective on hydrogen storage properties of MgH_2. The single phase rock salt formed after milling $2MgH_2$ +TiO_2 system for 30 h had the least dehydrogenation activation energy (110.9 kJ/mol). Further works of Pukazhselvan *et al.* (2017b) established that TiO_2 transformed as an inbuilt rock salt catalyst during dehydrogenation and its content depended on the variation of Mg/Ti. The proportion of Mg/Ti according to the researchers was assumed to cause e passivation of active rock salt. Shao *et al.* (2022) prepared three-dimensionally ordered macroporous (3DOM) TiO_2 via colloidal crystal template technique. After 10 h ball milling with MgH_2, the composite absorbed 4.17 wt.% H_2 at 100 °C within 1800 s and released 5.75 wt.% H_2 at 300 °C within 1000 s. Improvement in the hydrogen storage properties of MgH_2 arose from the combined effect of 3DOM structure and electronic interactions as TiO_2 was reduced by MgH_2 and multiple valence Ti (Ti^0, Ti^{1+} and Ti^{2+}) were formed. These destabilized MgH_2 and weakened Mg - H bonds. In addition, TiO_2 nanoparticles were wrapped and uniformly distributed in carbon layer; this aided de/absorption of hydrogen in MgH_2. Titanium and TiO_2, each of 0.4 g and 0.2 g of nitrogen-doped graphene (XFNANO) was ball milled for 1 h to obtain TiO@N-C (Hong *et al.* 2023). The additive (0.1 g TiO@N-C) was mixed with 0.9 g of MgH_2 and milled for 5 h. The composite completely desorbed hydrogen at 350 °C within 4 min and its dehydrogenated form absorbed 5.1 wt.% H_2 in 4 min at 175 °C. There was a reversible reaction of Ti and TiH_2 on Mg/MgH_2 surface during de/hydrogenation which made hydrogen molecules dissociate and diffuse easily; the stability of MgH_2 was also reduced by weakening of Mg - H bonds triggered by TiO_2. Nitrogen-doped graphene was covered on MgH_2 surface which impeded the agglomeration of MgH_2 particles. In addition, carbon structural defects that existed in nitrogen-doped grapheme acted as nucleation sites which promoted diffusion of hydrogen. These were responsible for the hydrogen storage performance of MgH_2. Multi-phase interface comprising Ti, TiO_2, Ti_2O_3 and MgH_2 has been established to provide more diffusion paths for hydrogen and more nucleation sites for Mg/MgH_2. This finding substantiates the investigations of Liu *et al.* (2021) who doped graphene-supported TiO_2 nanoparticles

(TiO_2@rGO) into MgH_2, Asides the fact that Mg was surrounded by the catalyst; partial reduction of Ti^{4+} to Ti^{2+} existed. This propelled charge transfer that advanced the de/hydrogenation kinetics of MgH_2. In addition, Ren *et al.* (2022) recorded that multi-phase interfaces that comprised multi-valence Ti (Ti^{2+}, Ti^{3+}) and MgH_2 existed when flower-like MgH_2/TiO_2 heterostructure synthesized from 2D TiO_2 nanosheets with oxygen vacancies. The multi-phases aided electron and hydrogen diffusion and created more nucleation sites for MgH_2/Mg. Magnesium rod, Ni sheet and Ti pellets were melted in a vacuum induction levitation furnace to process MgNi-Ti and MgTiNi ingots (Li *et al.* (2018). The alloy ingots were crushed and mechanically ground to 200-mesh powder. When milled, Ni_2Ti and NiTi phases were observed in both alloys. New phases- Mg_2NiH_4 and TiH_2 were formed after 100 cycles of hydrogenation and dehydrogenation. These phases were responsible for 5.22 and 3.23 wt.% H_2 recorded for MgNi-Ti and MgTiNi alloys, respectively. Amorphous $TiMgVNi_3$, produced via Induction melting of Ti, Ni and V powders, has been used as a catalyst on MgH_2 (Hu *et al.* 2022). After 100 h of milling, of cast $TiMgVNi_3$, 10 wt.% was further milled with MgH_2 for 10 h under 5 MPa H_2 pressure. Magnesium hydride and (Ti,Mg,V,Ni)H_x were formed after milling. When MgH_2/ $TiMgVNi_3$composite underwent 2 cycles of hydrogenation and dehydrogenation, a homogenous distribution of (Ti,V)H_2 and Mg_2NiH_4 nanoparticles formed on the surface of MgH_2; these were responsible for its fast hydrogen desorption Magnetic levitation melting has been used in preparing TiV based BCC alloy ($Ti_{0.4}Cr_{0.15}Mn_{0.15}V_{0.3}$) which was mechanically pulverized into particles as an additive for MgH_2 (Yu *et al.* 2010). Some alloy powders were water quenched while others were hydrogenated at 20 bars H_2 for 2 h at room temperature. Alpha -MgH_2, γ-MgH_2 and HBCC were formed after milling. The BCC contributed to the improvement of atomic diffusivity of hydrogen as well as its ease of dissociation and recombination. Hydrogenated BCC appeared to impart the most effective followed by quenched BCC. Solid BCC (ingot) offered the least effect. El-Eskandarany *et al.* (2019) milled MgH_2 with 10 wt.% $TiMn_2$ master alloy powders for 50 h under 70 bar H_2 pressure. The composite formed was further consolidated (compaction) into circular buttons of .1.2 and 8e2.0 cm diameter and thickness respectively. The consolidation enabled the $TiMn_2$ nanopowders got embedded in the micro/nanopores of MgH_2 grains which acted as a good hydrogen diffusion path during hydrogenation and dehydrogenation. The buttons could absorb and desorb 5.8 wt.% H_2 at 225 °C within short periods of 150 s and 500 s, respectively

Titanium carbide (TiC) nanoparticles was formed on the grain boundaries of MgH_2 when both underwent cryo-milling (using N_2 to enact freezing) for 8 h followed by high energy ball milling (at room temperature) for 16 h. (Tan & Shang, 2012). The formation of the additive on the grain boundary shortened the diffusion length and weakened the Mg-H bond which lowered the desorption temperature and activation energy to 190 °C and 235 to 104kJ/mol respectively. Sandwich-like Ti_3C_2/TiO_2(A)-C was processed via facile gas–solid approach and doped into MgH_2 by 10 h ball milling (Gao *et al.* 2020). X-Ray diffraction results showed that MgH_2, with few contents of Mg and MgO were formed after milling. From their investigation, incomplete hydrogenation or dehydrogenation of MgH_2 was suggested to have culminated in the formation of Mg while the reaction between MgH_2 and TiO_2resulted in the formation of MgO. The composite could absorb 5 wt.% H_2 at 250 °C within 1700 s (42.32 kJ/ moll) and within 800 s, 4 wt.% H_2 was desorbed at 125 °C (77.69 kJ/ mol). Multiple valence Ti compounds of Ti^{4+}, Ti^{3+}, Ti^{2+} and Ti^0 as observed by XPS and synergetic effects between the layered structure were reported to be the mechanism of the catalytic influence of Ti_3C_2/TiO_2(A)-C. A modified wet chemical method used in fabricating sandwich- like Ni/Ti_3C_2 catalysts, was introduced to MgH_2 to improve its hydrogen storage performance (Gao *et al.* 2021). A strong electronic interaction existed between nanoparticles of Ni and $Ti3C_2$. This was affirmed to be responsible for the improved hydrogen absorption feature of MgH_2. Catalytic effect of $NiTi_3C_2$ was influenced by the electron transfer in the multiple valences of Ti (Ti^{4+}, Ti^{3+}, Ti^{2+} and Ti^0). Works of Gao *et al.* (2021) justify earlier works (Cui *et al.* 2013) where it was claimed that $Ti3C_2$ derived its catalytic influence from electron transfer in multi-valence Ti which triggered the transformation of Mg^{+2} and Mg, H^- and H.

1.

3.2. Nickel (Ni)

A common Ni- based intermetallic compound – Mg_2Ni has been synthesized and reported over the years to be a good hydrogen storage material (Zaluski *et al.* 1995a; Zaluski *et al.* 1995b). Recently, Baroutaji *et al.* (2022) summarized that another Mg-Ni based compound - Mg_2NH_4 can be realized (together with Mg) when Mg_2Ni directly interacts with MgH_2. It can boost MgH_2 hydrogen storage feature when both materials interact (Lu *et al.* 2022). These two Mg-Ni based compounds have played important roles on MgH_2 hydrogen storage features and they can also be formed on reacting pure Ni or Ni- based compounds with MgH_2. Hanada *et al.* (2005) concluded that observing de/hydrogenation cycle of 2% mol Ni nanoparticle - doped MgH_2 at 200 °C, hydrogen desorption properties of the composite degraded as a result of Mg_2Ni which formed at that temperature. Here, the Ni content and/or the composite processing method (15 h ball milling under1 MPa H_2 pressure) may have been responsible for the limiting impact of Mg_2Ni. Using Ni in uncombined form could have also been responsible. It was reported by Liang *et al.* (2000) that milling Mg and 30 wt.% $LaNi_5$ intermetallic mechanically for as long as 40 h would not yield chemical reaction unless when hydrogenated. At this point, the intermetallic decomposed and a composite comprising MgH_2, LaH_3 and Mg_2NiH_4 phases was formed. When MgH_2 and 30 wt.% $LaNi_5$ were ball milled prior to hydrogenation, part of MgH_2 and $LaNi_5$ decomposed to form Mg_2NiH_4 while some part was reduced by La to form stable LaH_3 and Mg. After hydrogenation, MgH_2/ LaH_3/ Mg_2NiH_4 system similar to that observed on milling Mg powder with $LaNi_5$ was formed. Milling $LaNi_5$ with MgH_2 was preferable to Mg because the former facilitated ease of powder size reduction, which enhanced absorption properties of MgH_2 and not desorption. Magnesium absorption kinetics was improved by the presence of LaH_3; beyond 373 K, Mg_2Ni imparted a better catalytic effect. Hydrogen storage kinetics has been improved by doping MgH_2 with 5 wt.% SiC (Ranjbar *et al.* 2009a) but addition of 10 wt.% Ni further enhanced this property because it improved composite's surface area and reduced the concentrations of defects (Ranjbar *et al.* (2009b). In addition, hydrogen desorption reaction was influenced by bulk nucleation and 3D growth of the existing Mg nuclei; finely dispersed Ni nanoparticles increased the amount of nucleation sites.

Mao *et al.* (2010) ball milled MgH_2 with 10 wt.% $NiCl_2$ for 2 h. Magnesium hydride phase was observed after milling without a trace of Ni; this could be attributed to the little milling time employed or content of additive used. After hydrogenation and dehydrogenation cycles, more phases were formed which followed the suggested reaction:

$$3MgH_2 + NiCl_2 \rightarrow MgCl_2 + Mg_2Ni + 3H_2 \quad (1)$$

Magnesium chloride and Mg_2Ni acted as catalyst on MgH_2. It was also noted that the additive removed nucleation barrier which enabled hydrogen desorption occur at a low driving force. Within 60 s, 5, 17 wt.% H_2 was absorbed at 300 ^{0}C for $MgH_2/NiCl_2$ composite while it took 400 s to absorb 3.51 wt.% H_2 at the same temperature for undopped ball milled MgH_2. Furthermore, dehydrogenation activation energies of 158.5 and102.6 kJ/mol were calculated for MgH_2 and $MgH_2/NiCl_2$ composite respectively. Nano Ni powders produced via Ni carbonyl process was ball milled with high enthalpy MgH_2 (Wronski *et al.* 2011) Acting as a catalyst, the powders reduced desorption temperature of the metal halide as low as 100 ^{0}C at low hydrogen partial pressure The catalyst was affirmed to provide adequate surface area with carbon and oxygen (impurities formed during the carbonyl process) coating which was also responsible for activation energy reduction for hydrogen desorption. The activation energy for desorption reduced from 167 kJ/mol (unactivated MgH_2) to 78 kJ/mol for nano Ni-catalyzed MgH_2 between 325 – 350 ^{0}C. Cui *et al.* (2014) also reported that formation of Mg_2Ni improved the hydrogenation and dehydrogenation kinetics of Mg-Ni system. In their work, MgH_2 was ball milled with Ni nanoparticles which were uniformly dispersed and anchored on reduced graphene oxide (Ni@rGO) for 2, 5, 10 and 20 h under 1MPa H_2 pressure. A high surface area of 161.4 m^2/g possessed by Ni@C nanorods mixed with MgH_2 was investigated to absorb 6.4 wt.% H_2 within 10 min and 300 °C (An *et al.* 2014). Here, it was suggested that Ni@C composites had the capacity to create interface with MgH_2 to form catalytic site for hydrogen diffusion. When the combination of $SrTiO_3$ and Ni were used as additive for MgH_2 (Yanya & Ismail, 2018), Mg_2Ni and Mg_2NiH_4 were formed after dehydrogenation and hydrogenation respectively. The two phases were concluded to be active in improving the hydrogen storage properties of MgH_2. The phase $SrTiO_3$ remained unreacted throughout the process but its catalytic influence was imparted in the modification of the composite's microstructure. This created an additional advantage ahead of using only $SrTiO_3$. Nano Ni particles were dispersed in nanoporous carbon material (CMk-3) prepared by impregnation reduction and 10 wt.% of the combination was added to MgH_2 (Chen *et al.* 2018). Under 3 MPa H_2 pressure and 150 ^{0}C, the composite $MgH_2/Ni/CMk-3$ absorbed 3.1 wt.% H_2 after 360 s while 5.7 wt.% H_2 was absorbed with 2400 s. At 328 K, and 3 MPa, H_2 pressure, 3.9 wt.% H_2 was absorbed. Nickel nanoparticles played an active role in lowering the decomposition enthalpy of MgH_2 by forming Mg_2Ni and Mg6Ni. Combined effect of activation and destabilization from Ni was responsible for the enhanced performance of MgH_2. Ma *et al.* (2018) employed carbonization process to synthesize carbon supported nano-Ni (Ni@C) additive for MgH_2. Inclusion of 5 wt.% of the additive promoted MgH_2 the hydrogen storage display. After 10 cycles, average grain size of MgH_2 grew to 35.5 nm and this was reported to be responsible for its reduced storage capacity at that instant. Furthermore, Mg_2NiH_4 also appeared after 10 cycles and was suggested to have a negative impact on the composite's hydrogen performance. Increase in milling time up to 10 h has led to gradual reduction in crystallite and grain sizes of MgH_2/ nano Ni anchored on reduced graphene oxide (Ni@rGO) composite (Yao *et al.* (2020). On the other hand, prolong milling up to 20 h led to the welding and agglomeration of particles which made them bigger. Catalytic effect of the additive was influenced by the formation of Mg_2Ni/ Mg_2NiH_4 phase which was formed after rehydrogenation. Milling for 5 h offered the best result as the composite could absorb 5 wt.% H_2 in 20 min at 100 °C and within 15 min, 6.1 wt.% H_2 was released at 300 °C. It was easier for Mg_2NiH_4 to release H_2 with ease. The rGO created hydrogen diffusion channels and active catalytic site, which was responsible for the lowering of dehydrogenation temperature and kinetics. Solid solution of Ni-Cu powders has created a platform for enhanced MgH_2 nucleation and de/hydrogenation by reducing the bond strength of Mg-H (Zhang *et al.* 2020). At 300^0 C, the composite could eject 5.14 wt.% H_2 after 15 min while within 30 min, 4.37 wt.% H_2 was absorbed at 250 ^{0}C Magnesium hydride hydrogen storage display was elevated by the formation of $Mg_2Ni(Cu)$, which allowed hydrogen molecules to dissociate and recombine to MgH_2. Ball milling of Mg powder and $MgNi_2$ alloy followed by hydrogen combustion synthesis technique was devised by Fu *et al.* (2020) to synthesize $MgH_2/MgNi_2$ composite. Majority of the Mg were transformed to MgH_2 after hydrogenation while some reacted with $MgNi_2$ to form Mg_2NiH_4 that later transformed to Mg_2Ni during dehydrogenation. These two phases enhanced hydrogen adsorption and desorption of MgH_2 as 2.5 wt.% H_2 was absorbed at 200 °C while at 300 °C, 2.6 wt.% H_2 was released. Magnesium hydride was investigated to be capable of absorbing 5.3 wt.% H_2 at 300 ^{0}C within 5 min when doped with 2mol% nano Ni powders of approximately 90 nm via high pressure ball milling under 10 MPa H_2 pressure (Rahwanto *et al.* 2021). The nano Ni powders provided adequate reaction surface for MgH_2 during milling. Li *et al.* (2021) doped Ni/ Ni/tubular g-C_3N_4 (TCN) into Mg by milling for 5 h and under 4 MPa H_2 pressure, the milled sample was kept for 40 h to form $MgH_2/Ni/TCN$ composite. During milling, the additive coated the Mg surface and Ni particles reacted with Mg to form a phase that comprised Mg, Ni and H. The C atom, being a good conductor of heat and electron, was considered good for the behavior of the composite when hydrogenated and dehydrogenated at 400 °C; it also prevented the growth of particles. Reversible conversion from Mg to MgH_2 and reaction between Mg_2NiH_4 and $Mg_2NiH_{0.3}$ were realized during de/hydrogenation of the composite. The C coating on Mg and the formation of Mg-Ni-H phases (Mg_2NiH_4 and $Mg_2NiH_{0.3}$) improved the hydrogen storage properties of MgH_2. Tricarboxybenzene was used by Shao *et al,* (2021) to process Ni-MOF (N- BTC300), which was calcined at 300 °C as catalyst for MgH_2. The additive displayed uniformly dispersed and bonded metal ions which improved the hydrogenation and dehydrogenation kinetics of MgH_2. With the addition of 10 wt.% Ni-MOF, composite could release 5.14 wt.% H_2 at 300 °C. This was better than additive free MgH_2 that released 0.09 wt.% H_2 after 15 min at the same temperature. Good cyclic behavior of composite was attributed to the robust structure of MOF. Rods of Ni – based oxide, $NiMoO_4$ was incorporated into MgH_2 by 6 h ball milling (Huang *et al.* 2021). The composite still contained $NiMoO_4$ and MgH_2 after milling while Mg, Mo, MgO and Mg_2Ni phases were formed after complete desorption at 300 °C, which indicated that $NiMoO_4$ reacted with MgH_2 in the process according to the reaction:

$$6MgH_2+NiMoO_4 \rightarrow Mg_2Ni + 4MgO + Mo + 6H_2 \quad (2)$$

Magnesium hydride$_2$ and Mg_2NiH_4 were formed after hydrogenation at 150 ^{0}C and 3.2 MPa H_2 pressure. Within 10 min, $MgH_2/NiMoO_4$ was able to desorb 6 wt.% H_2 at 300 °C and adsorb 5.5 wt.% H_2 at 150 °C after 10 min. The exceptional de/hydrogenation kinetics was ascribed to the formation of Mg_2Ni and Mo after reaction of MgH_2 with $NiMoO_4$ while Mo° encouraged the removal of hydrogen atoms from MgH_2 under less severe ball milling. A reversible phase evolution among Mg_2Ni,Mg_2NiH_4 and $CeH_{2.73}$ was reported to exist after hydrogenation and dehydrogenation of ball milled $Ni@CeO_2/MgH_2$ composites (Yu *et al.* 2023) These phases

enhanced the hydrogen storage properties of MgH_2 as they were finely dispersed in its matrix.

3.3. Vanadium (V)

Mechanically ball milling MgH_2 with V for 20 h was observed to yield βMgH_2, γMgH_2 and $VH_{0.81}$ after hydrogenation (Liang *et al.* 1999). Hydrogen was completely desorbed after 2000 s at 800 K with MgH_2/5 wt.% V. The nanocomposite absorbed 2 wt.% H_2 within 1000 s at 10 MPa H_2 pressure and 302 K; at 373 K, 4 wt.% H_2 was absorbed after 100 s and at 473 K, 6.5 wt.% H_2 was absorbed in 250 s. The microstructure of composite with V inclusion improved the hydrogenation kinetics. Vanadium (5 wt.%) was added to MgH_2 powders and mechanically ball-milled for 100 h to nano scale (Rivoirard *et al.* 2003). At 253 K MgH_2 absorbed hydrogen slowly while that activated with V was faster. Fine grains of MgH_2 formed were also responsible for its enhanced hydrogen absorption kinetics. At 603 K the absorption kinetics was reduced because it was noticed that at that temperature, δVH_x which was formed after ball milling became unstable. They concluded that nature of combining materials would not only contribute to hydrogen absorption properties of MgH_2; particle size reduction, distribution and agglomeration would also play key roles. After mechanically milling Mg and V powders for 20 h, $MgV_{0.05}$ was formed and this improved the hydrogen storage property of Mg (Schimmel, *et al.* (2005). At the onset of hydrogenation, $MgH_{1<x<2}$ phase was formed and there was much hydrogen vacancies which enabled the phase have higher diffusion coefficient. This was responsible for the improved hydrogenation kinetics of the nanocomposite. Conceição *et al.* (2014) compared the effects of pure V, vanadium chloride (VCl_3) and vanadium carbide (VC) catalysts on the hydrogen storage properties of MgH_2. Adding 5 wt.% separately of each additive to MgH_2, VCl_3 showed the best catalytic effect in terms of hydrogen storage capacity and de/hydrogenation kinetics. It was reported that considering the same content for all additives (wt.%), the amount of V in VCl_3 was the least compared to that in VC and pure V. Vanadium carbide could enhance desorption of MgH_2 but its high stability contributed to its retarded desorption kinetics. According to Kadri *et al.* 2(015), catalyzed V synthesized from vanadium hydride, VH_2 could act as a hydrogen splitting agent which could hasten dissociation of hydrogen from MgH_2. Catalytic influence of bismuth vanadate ($BiVO_4$) on MgH_2 hydrogen storage properties via ball milling has been investigated (Xu *et al.* 2017). At 150 °C, and 3 MPa H_2 pressure, the composite composed of MgH_2/16.7 wt.% $BiVO_4$ had the capacity to absorb 1.99 wt.% H_2 while additive-free MgH_2 had 0.94 wt.% H_2 absorbed under the same conditions of temperature and pressure (Figure 5a). At 400 °C, 1.1 wt.% H_2 was desorbed within 1200 s (Figure 5b). Catalytic influence of $BiVO_4$ was attributed to the formation of V-containing compounds ($Mg_2V_2O_7$ and V_2O_3) that were formed during dehydrogenation at 400 °C.

Vanadium oxide supported on cubic carbon nanoboxes (nano-V_2O_3@C) has been ball milled with MgH_2 (Wang *et al.* 2018). Within 10 min, MgH_2/-9 wt.% V_2O_3@C composite could release 6.0 wt.% H_2 while additive – free MgH_2 desorbed 0.4 wt.% H_2 within this time. The metallic V formed from V_2O_3 during milling and at the initial stage of heating was responsible for the fast dehydrogenation kinetics of MgH_2; it elongated Mg - H bond length and weakened its strength. Vanadium chloride was reduced to metallic V when milled with MgH_2 Kumar *et al.* (2018). The metallic V imparted a good catalytic effect on MgH_2 hydrogenation and dehydrogenation kinetics. This was achieved by MgH_2 grain refinement and crystallite size reduction that eventually created the diffusion path for hydrogen. In the investigations of Liu *et al.* (2021), 7 wt.% of V nanoparticles was added to MgH_2. Within 10 min, 6.5 wt.% H_2 was released at 300 °C (MgH_2 could not achieve this at this time). Fully dehydrogenated composite had the potency of absorbing hydrogen at room temperature and 5.6 wt.% H_2 at 150 °C. Vanadium remained stable all through hydrogenation and dehydrogenation processes. Well dispersed Ni and vanadium trioxide nanoparticles in nanoporous carbon ((Ni-V_2O_3)@C) has been used as catalyst on MgH_2 (Lan *et al.* 2022). There was a partial transformation of V_2O_3 to VO during milling while MgH_2, V_2O_3, VO, and V remained unreacted during hydrogenation and dehydrogenation. In contrast, Ni reacted with Mg to form Mg_2Ni and this further reacted with hydrogen to form Mg_2NiH_4. The Mg_2Ni/ Mg_2NiH_4 particles acted as hydrogen pump as it was observed to be coated on Mg/MgH_2; this aided diffusion and dissociation of hydrogen The presence of carbon (C) enhanced the catalytic effect, promoted MgH_2/Mg lattice expansion and held up their crumbling during hydrogen de/absorption, which ended improving MgH_2 cyclic stability. It was concluded that m a multicomponent catalyst comprising V, VO, V_2O_3, C, and Mg_2Ni/Mg_2NiH_4 will improve the hydrogen

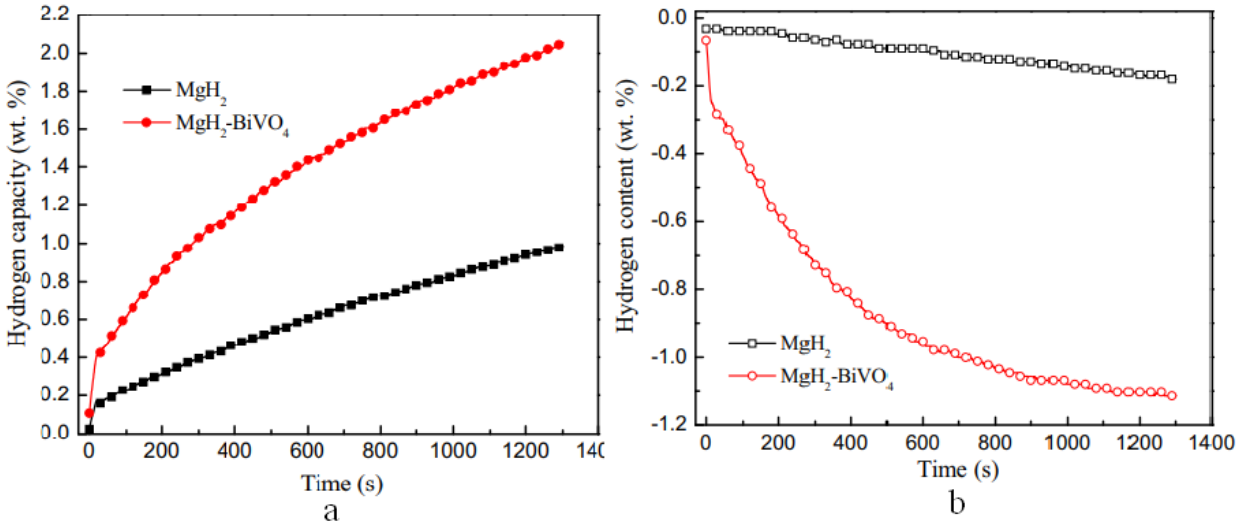

Fig 5. (a) Hydrogen absorption of additive-free milled MgH_2 and at MgH_2/ 16.7 wt.% $BiVO_4$at 23 K.(b) Hydrogen release of MgH_2 and at MgH_2 /16.7 wt.% $BiVO_4$at 523 K (Xu *et al.* (2017).

performance of MgH_2. Two dimensional canadium carbide (V_2C) MXene has been added to MgH_2 to improve its hydrogen desorption kinetics (Lu *et al.* 2022). Improved cyclic stability was not only caused by the additive; low hydrogen desorption temperature (from 318 ^{0}C in MgH_2 to 198 ^{0}C in MgH_2/V_2C composite) was also enhanced. The V_2C played a role of reducing Mg H bond length to hasten desorption kinetics of MgH_2. Tian *et al.* (2023) ball milled hydrothermally synthesized V- based catalysts (V_2O_5, $FeVO_4$and NiV_2O_6) with MgH_2. to improve its hydrogen storage properties. Dehydrogenation behaviour of MgH_2/ $FeVO_4$ displayed the best performance followed by MgH_2/V_2O_5. During this process, the Fe-V complex oxide reduced elemental Fe and V which eventually lowered Mg-H bond strength. This hastened the absorption and desorption of MgH_2.It was concluded that Fe would improve the catalytic effect of V_2O_5 while Ni will not. Structured V- based MOFs (MOFs-V) synthesized by facile hydrothermal reaction and calcination has been doped with MgH_2 via ball milling to modify its hydrogen storage properties (Lu *et al.* 2023). It was observed by Scanning Electron Microscope (SEM) that the MOFs composed of bullet-like V_2O_3. The desorption temperature of composite containing 5 wt.% MOFs was 199.8 ^{o}C which was 142 ^{o}C lower than catalyst-free MgH_2; increasing the content of MOFs to 7 and 9 wt.% further lowered the desorption temperatures to 190 and 186 ^{o}C respectively. During ball milling, MOFs-V was reduced to metallic V which created a catalytic effect. Catalytic effect of vanadium disulphide (VS_2) on MgH_2 was investigated by Verma *et al.* (2023). The composite began to release hydrogen at 289 ^{o}C which was 87^{o}C lower than MgH_2. Hydrogen desorption activation energy barrier required to reduce MgH_2 to Mg in the presence of VS_2 was lower (98.09 kJ/mol) compared to42 kJ/mol in catalyst-free MgH_2. Du *et al.* 1(997) had earlier reported that V in VS_2 could be reversibly converted from V^{4+} to V^{5+} during de/hydrogenation. The existence of V in its variable oxidation form would weaken Mg-H bond and thus trigger fast de/hydrogenation kinetics.

3.4. Molybdenum (Mo)

Jia *et al.* (2013) reported that molybdenum disulphide (MoS_2) had more effect in improving the absorption and desorption kinetics of MgH_2 than molybdenum oxide (MoO_2). During ball milling, the following reactions were investigated to have taken place as indicated from XRD patterns:

$$2MgH_2(s) + MoS_2(s) \rightarrow 2MgS(s) + Mo(s) + 2H_2(g) \quad (3)$$

$$2MgH_2(s) + MoO_2(s) \rightarrow 2MgO(s) + Mo(s) + 2H_2(g) \quad (4)$$

Considering similar ball milling conditions, reaction (3) was observed to be faster than reaction (4). As-milled MgH_2 could absorb 90% of its hydrogen storage capacity within 72 min; MgH_2/MoO_2 could attain this within 31 min while it took 13 min for MgH_2/MoS_2 to achieve this. Formation of MgS/ Mo and MgO/Mo in each reaction was suggested to have been responsible for the absorption/desorption kinetics of MgH_2. Addition of 10 wt.% MoS_2 to Mg particles according to Han *et al.* (2016) would be enough to prevent agglomeration and cold welding of particles as it acted as a dispersant and lubricant. The milling process reduced crystallite size of MgH_2 to a little below 38.8 nm and this was sustained all through milling because MoS_2 confined its growth. The reduction in crystallite size was responsible for the reduced dehydrogenation temperature of MgH_2. During MgH_2 decomposition, crystal of Mg was reported to grow by three dimensions controlled by interface transformation. The researchers concluded that MoS_2 had a weak catalytic influence on the decomposition of MgH_2. Rather than use bulk MoS_2, Setijadi *et al.* (2016) synthesized MgH_2 nanoparticles using delaminated MoS_2 through a simple hydrogenolysis route which involved the decomposition of di-n-butylmagnesium. The delaminated additive led to the formation of Mg worm-like structures that collapsed and recrystallized during hydrogen cycling. Thermodynamic features of Mg/MgH_2 reaction was strongly influenced by the additive through destabilization of the Mg-H bond.

Han *et al.* (2017) observed that after ball milling Mg/C (combination of magnesium and crystalline carbon) with Mo for 3 h under 1 MPa H_2 pressure, MgH_2 was formed. Molybdenum and crystalline carbon offered a synergistic effect on improving the hydrogenation kinetics of MgH_2 in the reactive ball milling process. Enhanced dehydrogenation rate of MgH_2 was attributed to the conductive capacity of Mo The use of 2% mol. MoO_3 was researched to have a positive impact on hydrogen storage performance of MgH_2 (Dan *et al.* 2019). During hydrogenation and dehydrogenation, MoO_3 was an active site for hydrogen absorption and desorption; the oxide was observed to also create a fast diffusion pathway for hydrogen atoms. Formation of MoO_2 occurred during hydrogenation (reduction of MnO_3 to MnO_2), which was affirmed to reduce the catalytic effect of MoO_3 on the long run. Synthesized nanosheets of $NiMoO_4$ were ball milled with MgH_2 (Chen *et al.* 2020). After activation, MoNi and Mg_2Ni nanoparticles were formed, which created reaction surfaces and hydrogen diffusion channels. Synergic effects of MoNi on MgH_2 increased hydrogenation and dehydrogenation kinetics than the use of mono atomic Mo and Ni on MgH_2. The MoNi possessed high hydrogen absorption capacity which was able to dissociate hydrogen from MgH_2 by breaking Mg-H bonds. Magnesium hydride has been separately milled with 10 wt.% $MoSe_2$@$FeNi_3$ hollow nano-spheres, $FeNi_3$, and $MoSe_2$ particles (Gao *et al.* 2020). All additives showed improved catalytic influence on the hydrogenation and dehydrogenation reactions of MgH_2 but $MoSe_2$@$FeNi_3$ offered the best performance. The combination of $FeNi_3$, and $MoSe_2$ was responsible to its excellent catalytic performance. Dehydrogenation of 10 wt.% $MoSe_2$@FeNi3-doped MgH_2 composite commenced from 194 ^{o}C; it could absorb 5.8 wt.% H_2 within 0.5 min at 150 ^{o}C. The combined additive propitiated the formation of active MgSe, Fe, Mg_2Ni and Mo species that were uniformly distributed on the surface of MgH_2. They were reported to have engendered the de/hydrogenation stability of MgH_2. Furthermore, Mg_2Ni turned MgH_2 to an effective pathway for hydrogen absorption and desorption. Molybdenum flakes have been used in improving the hydrogen storage capacity of MgH_2 (Cheng *et al.* 2023). Adding 7 wt.% Mo flakes to MgH_2 powder, hydrogen desorption commenced at 250 ^{0}C, which was 100^0 C lower than ordinary MgH_2 (350^{0}C). The composites released 6.5 wt.% hydrogen for 20 min at 325 ^{0}C. At room temperature, the composite began to absorb hydrogen and 6 wt.% was absorbed at 250 ^{0}C within 10 min. Lamellar surfaces possessed by the flakes provided more diffusion pathways and contact surfaces which hastened diffusion of hydrogen at Mg/MgH_2 interfaces. Molybdenum remained stable during de/hydrogenation cycles and this made it impart an active catalytic effect on MgH_2.

3.5. Chromium (Cr)

Prolonged hydrogenation-dehydrogenation cycling was devised by Dehouche *et al.* (2002) to determine the thermal stability of MgH_2/0.2 mol % Cr_2O_3 naocomposite. At 350 ^{0}C, the composite possessed the best absorption kinetics after 17 cycles and it witnessed the least kinetics after 1000 cycles at 300 ^{o}C. Absorption rate of 47 kW/kg was maintained at 300 ^{o}C after 1000 cycles while desorption rate reduced to 4.5 kW/kg. During the cycling process, the crystallite size which was initially 21 nm

grew to 84 nm after 1000 cycles at the same temperature; the coarsening of the composites microstructure was responsible for the slow desorption rate. Coarsening of the microstructure was maintained up to 350 °C. Cycling effects on MgH_2 /10 wt.% Cr_2O_3 nanopowder composites was studied by Polanski *et al.* (2011). At 325 °C, the ball milled nanocomposite was put through 150 de/absorption cycles. Progressive reduction of nanocomposite's hydrogen storage capacity was witnessed after every 25 cycles; this ranged from 5.1 wt.% H_2 after the 1st cycle to 4.6 wt.% H_2 on the 150th cycle This reduction in nanocomposite's hydrogen storage capacity upon cycling was ascribed to the formation of agglomerates that arose from the sintering (as a result of long term cycling) of combining powders (MgH_2 and Cr_2O_3), reduction of Cr_2O_3 to Cr with formation of MgO and existence of Cr_2O_3 particles in Mg interface. Bimetallic Cr-V was confirmed effective for hydrogen sorption kinetics of MgH_2.within room temperature and 300 °C (Zahiri *et al.* 2011).Within 1 h, 5 wt.% H_2 was absorbed at room temperature and 2 bar; the composite remained stable beyond 225 cycles with reduced degradation kinetics at 200 and 300 °C. The stability was attributed to positioning of nanocrystalline bimetallic Cr-V catalyst at Mg/MgH_2 grain boundaries which ended up coating the surface. With increasing cycling, the coating potency of Cr-V was dwindled and limited the cycling stability of MgH_2/Cr-V composite.

3.6. Iron (Fe)

Iron is regarded as an inexpensive and the most abundant transition metal on earth (Du *et al.* 2015). Several studies have proven that Fe can upgrade the hydrogen storage properties of MgH_2 in its pure form, as an alloy/compound and in composite with other materials. Yavari *et al.* (2005) ball milled MgH_2 with 3 wt.% iron (III) fluoride (FeF_3) nanoparticles. There was a partial transfer of fluorine (F) which formed protective intergranular MgF_2 with fine dispersed Fe nanoparticles in Mg or MgH_2 according to equation (5). The catalytic effect could have come from the Fe formed.

$$3MgH_2 + 2FeF_3 + 3MgF_2\,(\text{intergranular}) + 2Fe + 3H_2 \quad (5)$$

Bassetti *et al.* (2005) reported that when MgH_2 was ball milled with Fe particles in ball to powder ratios (BPR) of 1:1, 3:1 and 10:1, MgH_2, MgO and Mg were formed. When BPR was increased to 20:1, additional phase Mg_2FeH_6 was formed. Optimum microstructure that showed a uniform distribution of micron and submicron-sized Fe particles in the MgH_2 matrix was achieved at high milling energy (BPR of 10:1 and 20:1). Also, 10 wt.% Fe was the optimum catalyst concentration because contents lower than this led to the formation of poorly catalyzed regions; concentrations beyond this value yielded no improvement either. Ten weight percent of Fe and Iron (III) oxide (Fe_2O_3) were separately ball milled with MgH_2 for 3 h under 0.3 MPa H_2 pressure (Baum *et al.* 2007). Although mechanism of the improved ad/desorption properties of MgH_2 was not fully established, Fe acted as an active site for hydrogen sorption (Fe_2O_3 was also reduced to Fe). Iron (III) oxide displayed a better catalytic effect. It could be assumed here that a more reduced crystallite size offered by Fe_2O_3 may be responsible for this. Santos *et al.* (2014) discovered that using elemental Fe nanoparticles would give a better catalytic effect on $MggH_2$ hydrogen sorption performance than nanoparticles of FeNb (ferroniobium) alloy. During milling, it was observed that nanointerfaces comprising Mg (MgH_2)/Fe and Mg (MgH_2)/FeNb alloy were formed which acted as diffusion paths for hydrogen into the bulk particle. These interface according to the researchers, possessed high chemical interfacial energies. Formation of NbO_2 and Nb_2O_5 when milled with the alloy may have been responsible for its lower sorption kinetics. The catalytic effect of as-synthesized graphene sheet templated Fe_3O_4 nanoparticles (Fe_3O_4@GS) on MgH_2 was examined by (Bhatnagar *et al.* 2016). The structure of as milled composite (MgH_2/ Fe_3O_4@GS) contained MgH_2, Fe, Fe_2O_3, MgO and $Mg_{1-x}Fe_xO$. Graphene sheet prevented the agglomeration of Fe nanoparticles (formed by reduction of Fe_3O_4), increased the surface area, durability and cycle stability (after 25 cycles of de/hydrogenation) of MgH_2. It was investigated that the layer of MgO was punctured by Mg_xFe_xO which created hydrogen diffusion pathway through its layer. In addition, electron transfer between Mg^+ and H^- during de/hydrogenation was engendered by the multiple valence of Fe. Surfactant-assisted solvothermal method was used in preparing FeS_2 micro-spheress which was ball milled with MgH_2 (Zhang *et al.* 2018). Adding 16.7 wt.% of the additive, the following reactions were confirmed to have taken place after milling:

$$2MgH_2 + FeS_2 \rightarrow 2MgS + Fe + 2H_2 \quad (6)$$

$$2MgH_2 + Fe + H_2 \rightarrow Mg_2FeH_6 \quad (7)$$

4. After hydrogenation at 350 °C, MgH_2 and Mg_2FeH_6 appeared as the major phases while their decomposition yielded metallic Mg and Fe after dehydrogenation at the same temperature. The composite could release 1.24 wt.% H_2 at 350 °C within 1400 s while pure MgH_2 could release 0.18 wt.% H_2 under similar condition. The composite absorbed 3.71 wt.% H_2 within 1400 s at 250 °C, compared with 1.03 wt.% H_2 of the as-milled pure MgH_2. Mg_2FeH_6 and MgS created diffusion pathway for H_2 diffusion. Sazelee *et al.* (2018) confirmed that MgO, Fe and Ba were formed after milling MgH_2 with 10 wt.% $BaFe_{12}O_{19}$ and these imparted synergic effects on hydrogen storage properties of MgH_2. Onset decomposition temperature for composite was 270 °C while as-milled MgH_2 was 340 °C. At 150 °C, its absorption capacity was 4.5 wt.% H_2 after 10 min while for the additive-free MgH_2, it was 3.5 wt.% H_2. The composite could release 4.2 wt.% H_2 in 30 min while additive-free MgH_2 could do that 3.4 wt.% H_2within the same time. Iron based MOFs has been synthesized and introduced to MgH_2 by ball milling. (Ma *et al.* 2019). The improved hydrogen storage of the composite was ascribed to the formation of nano α-Fe particles which was uniformly distributed on de/hydrogenated Mg/MgH_2 surface. Ball milling was employed in creating homogenous dispersion of the individual catalyst: Fe, Fe_2O_3 and $Fe3O_4$ in MgH_2 powders (Gattia *et al.* 2019). Activation energy for decomposition as calculated by Kissinger plots showed that 10 h ball milled MgH_2/5 wt.% Fe possessed the least magnitude of 220.69 kJ/mol. Vales recorded for MgH_2/5 wt.% Fe_2O_3 and MgH_2/5 wt.% Fe_3O_4 were 231.90 and 304.45 kJ/mol respectively. Low activation energies maintained using Fe and Fe_2O_3 compared to that of uncatalyzed MgH_2 (241.46 kJ/mol) indicated that these two materials gave good catalytic effects on desorption kinetics of MgH_2. Gao *et al.* (2019) doped MgH_2 with 10 wt.% iron boride (FeB) by dry milling and wet milling (with cyclohexane) at room temperature. Both milling techniques improved the hydrogenation and dehydrogenation performance of MgH_2 compared to additive-free MgH_2 as the *in situ* formed Fe and B served as active species during the process. Wet milling yielded smaller particles than dry milling and this was responsible for its better performance. Iron nanosheets have been synthesized to act as catalystt on MgH_2 (Zhang *et al.* 2019). Adding 5 wt.% Fe nanosheets made the activation energy for the dehydrogenation reaction to be 40.7 kJ/mol, which was 85.2 kJ/mol lower than the catalyst- free MgH_2. Within 10 min, 6 wt.% H_2 was absorbed by the composite at 200 °C while 2.3 wt.% H_2 was taken up after 45 min at the same temperature. It was noticed that during the first

hydrogenation and dehydrogenation processes, the Fe nanosheets became ultrafine nanoparticles on MgH_2; this created more active sites in the cycles that followed. At the onset of adding Fe nanosheets, Mg-H bond was broken. Catalytic influence of nanostructured Fe_7S_8 (pyrhotite) on hydrogen sorption properties of MgH_2 was studies by Cheng *et al.* (2021). Doping the parent hydride with 16.7 wt.% Fe_7S_8 and ball milling, 4 wt.% H_2 was absorbed at 200 °C within 1800 s; undoped MgH_2 had the capacity to absorb 1.847 wt.% H_2 at the same temperature and time. Also, within 1800 s and 350 ^{0}C, 4.403 and 2.479 wt.% H_2 were released by MgH_2/Fe_7S_8 composite and MgH_2 respectively. The Fe_7S_8 catalyzed MgH_2 composite began to desorb hydrogen at a much lower temperature (147 °C) compared to as milled MgH_2 (437 °C), Improvements on the hydrogen storage performance of MgH_2 by the catalyst was credited to the formations of MgS and Fe from the reacting materials that occurred during ball milling. Synthesized Fe nanoparticles were ball milled with MgH_2 to tailor its hydrogen storage performance (Song *et al.* (2022). Magnesium hydride remained dominant after ball milling and hydrogenation while Mg phase was formed in the dehydrogenated phase. The existence of stable Fe in the three stages was responsible for the enhanced absorption and desorption of Mg/MgH_2 system as it acted as an active catalytic site during these processes. The composite retained 93.4% of its hydrogen capacity after the 20th cycle. At this point, grain growth in MgH_2 and Fe catalyst occurred which was responsible for capacity loss and kinetics reduction. Soni *et al.* (2023) reported effect of Fe nanoparticles and hollow carbon spheres composite on the hydrogen storage properties of MgH_2. During hydrogenation and dehydration cycles, the valence state of Fe was converted from +3 to +2 and this was responsible for the improved hydrogen storage properties of MgH_2.

3.7. Cobalt (Co)

The modification of MgH_2 hydrogen sorption potency has been achieved by doping with combined oxides of Co and Ni (Cabo *et al.* 2011). Addition of 5 wt.% mesoporous NiO increased the desorption rate 7 times greater than MgH_2 with reduced sorption activation energy. Addition of nanoporous Co_3O_4 showed a minimal improvement while nanoporous $NiCo_2O_4$ imparted property that was in between MgH_2/NiO and MgH_2/ Co_3O_4. The role of $CoFe_2O_4$ nanoparticles on the dehydrogenation of MgH_2 was demonstrated by Shan *et al.* (2014). Ball milled MgH_2/ 7 mol% $CoFe_2O_4$ composite began to desorb hydrogen at 160 °C and this was 200 °C less than the onset desorption temperature of additive-free MgH_2. It was observed that during dehydrogenation, $CoFe_2O_4$ reacted with MgH_2 to form a ternary combination of Co_3Fe_7, MgO and Co; these were affirmed to catalyze the decomposition of MgH_2. Hierarchical Co@C nanoflowers have been reported to create more hydrogen diffusion channels and active catalytic sites that aided the reduction of hydrogen desorption temperature of MgH_2 (Li *et al.* 2017). The hierarchical Co@C nanoflowers were synthesized by employing a simple route that was based on a low temperature solid-phase reaction; it was milled with MgH_2 for 5 h under 1 MPa H_2. Onset desorption temperature of the composite (201 °C) was 99 °C lower when compared with as-milled MgH_2. Within 30 min, the composite released 5.74 wt.% H_2 within 30 min and at 300 °C , 6.08 wt.% H_2 was released in 60 min. On the other hand, as-milled MgH_2 could release 0.37 wt.% H_2 within 30 min; at 300 °C, 1.20 wt.% H_2 was released in 60 min. Gao *et al.* (2020) used 10 wt.% CoFeB/CNTs as an additive to improve de/hydrogenation behaviours of MgH_2. This was actualized by *in situ* formed stable Co_3MgC, Fe, CoFe and B which created active nucleation sites for de/hydrogenation reactions. In addition to the formation of these phases, uniform distributions of Co, B, Fe and C in the composite contributed to its good cyclic stability. Hydrolysis of MgH_2 in the presence of 2.5 – 10 wt.% $CoCl_2$ to produce hydrogen was executed by Filiz (2021). It was concluded that the best performance in terms of kinetics of hydrogen generation was displayed using $CoCl_2$ solution with a concentration of 6.55 wt.%. Core-shell CoNi@C bimetallic nanoparticles (MOFs) were introduced to MhH_2 to improve its hydrogen storage properties (Zhao *et al.* 2021). During dehydrogenation, Mg_2Co and Mg_2Ni were formed as the composite desorbed 5.83 wt.% H_2 at 275 °C within 1800 s. During hydrogenation, Mg_2Co and Mg_2Ni were transformed to Mg_2CoH_5 and Mg_2NiH_4. The composite could absorb 4.83 wt.% H_2 within 1800 s at 100 °C. Hydrogen dissociation and recombination were hastened as a result of the reversible phase transitions of Mg_2Co/ Mg_2CoH_5 and Mg_2Ni/Mg_2NiH_4. Heat conduction during the thermal cycles was facilitated by the good thermal conductive feature of carbon and this hindered agglomeration of nanoparticles. Carbon also provided a confinement effect which also aided the stability of MgH_2 during de/hydrogenation cycles. Ali *et al.* (2022) doped MgH_2 with 10 wt.% $CoTiO_3$. Hydrogen was desorbed at 270 °C, which was lower than that of MgH_2 that occurred at 340 °C. Within the first 10 min, 6.4 wt.% H_2 was adsorbed. Activation energy of MgH_2 was measured to be 135 kJ/mol while on adding $CoTiO_3$, it reduced to 104.6 kJ/mol. *In situ* formation of $MgTiO_3$, $CoMg_2$, $CoTi_2$, and MgO formed during heating elevated the hydrogen storage performance of MgH_2. Clusters of Mg_2NiH_4/Mg_2CoH_5 interfaces were reportedly formed after mechanically milling MOF-derived bimetallic Co@NiO catalyst with MgH_2 for 6 h (Zhang *et al.* 2022a). The interfaces were formed on the surface of MgH_2 and they were confirmed to create low energy barrier hydrogen diffusion channels which culminated in rapid release and uptake of hydrogen. Zhang *et al.* (2022b) doped Co particles into MgH_2 via 2 h ball milling. Cobalt particles were uniformly distributed on the surface of MgH_2 and this created active sites and paths for hydrogen diffusion. De/hydrogenation kinetics of MgH_2 was hastened as a result of Mg_2Co/Mg_2CoH_5 phase change that existed during hydrogenation and dehydrogenation. When 10 wt. % $CoMoO_4$/rGO nanosheets was milled with MgH_2 for 4 h (Zhang *et al.* (2022c), these three components - Mo, Co_7Mo_6 and MgO were formed. They had a synergic catalytic effect on improving the hydrogen storage capacity of MgH_2. The composite began to release hydrogen at 204 °C, while as-milled MgH_2 commenced desorption at 330 °C. The combined catalytic effect of the generated components was also responsible for accelerated hydrogen diffusion.

3.8. Zirconium (Zr)

Hydrogen storage features of MgH_2 separately catalyzed with 7 wt.% ZrF_4 and NbF_5 after series of cyclic loading were researched by Malka *et al.* (2011). At 325 °C, MgH_2/ZrF_4 maintained 5 wt.% H_2 after 30 cycles while MgH_2/NbF_5 could hold 4.5 wt.% H_2; thus implied that the former composite possessed a better hydrogen sorption stability at this temperature. Existence of stable ZrF_4 nanoparticles in the structure of MgH_2 was found responsible for a better hydrogen storage capacity. Reduction in the stability of MgH_2/ZrF_4 however was attributed to the gradual grain size increase by virtue of extended number of cycling. At this point, it was reported that more stable MgH_2/Mg phases were formed and contributed to formation of large grain sizes. Shahi *et al.* (2015) introduced $ZrFe_2$ and its hydride ($ZrFe_2H_x$) to investigate hydrogenation features of MgH_2 by producing $MgH_2/ZrFe_2$ and MgH_2/ $ZrFe_2H_x$ nanocomposites after milling. Intermetallic

$ZrFe_2$ was converted to fine powders of $ZrFe_2H_x$ via hydrogenation; it was noted to be a more useful catalyst as it was more homogenously distributed after milling. Desorption temperatures for as received MgH_2, $MgH_2/ZrFe_2$ and $MgH_2/ZrFe_2H_x$ were 410, 368 and 290 °C respectively. At 280 °C and 2MPa H_2 pressure, ball-milled MgH_2 could absorb 4.5 wt.% H_2 after 1 h while $MgH_2/ ZrFe_2$ and $MgH_2/ ZrFe_2H_x$ nanocomposites could absorb 4.6 and 5.2 wt.% H_2 respectively under the same condition.; it was further confirmed that $MgH_2/ ZrFe_2H_x$ absorbed 4.7 wt.% H_2 within the first 20 min. The catalyst hydride was also found to be responsible for a reduced activation energy (61.4 kJ/mol) because it facilitated easy dissociation of hydrogen molecules to atoms and transferred it to it to Mg/ZFe2H_x. Kumar *et al.* (2027) reported that when $ZrCl_4$ was used as a catalyst in improving on hydrogen sorption kinetics of MgH_2 via milling, metallic Zr or $ZnCl_3$ was formed. Either phase according to the researchers modified the surface of MgH_2 which was responsible for its hydrogenation and dehydrogenation kinetics. Activation energies of 40 and 92 kJ/mol were recorded for $MgH_2/ZnCl_4$ hydrogenation and dehydrogenation respectively while 70 kJ/mol (hydrogenation) and 150kJ/mol (dehydrogenation) were 0bserved for catalyst-free MgH_2. Refined grains possessed by catalyzed MgH_2 (via the use of $ZnCl_4$) was also noted to be responsible its improved hydrogenation and dehydrogenation kinetics. The refinement of grains occurred during ball milling and dehydrogenation. The product ZH_x/MgO nanoparticles were confirmed to be formed after ball milling of MgH_2 and ZrO_2 for 20 h (Pukazhselvan *et al.* 2022). This phase was known to be responsible for the improvement of MgH_2 sorption kinetics and stability.

3.9. Niobium (Nb)

A metastable NbH was formed by the hydrogenation and dehydrogenation of Mg from a 20 h ball milled MgH_2/5 wt.% Nb composite (Huot *et al.* 2003). The formation of NbH decreased the energy barrier for MgH_2 dehydrogenation. Effects of cyclic heating on milled MgH_2/2mol% Nb_2O_5 was carried out by Friedrichs *et al.* (2006). After hydrogen had desorbed from MgH_2, Nb_2O_5 was reduced to Nb; dissociated Mg reacted with oxygen from the additive (Nb_2O_5) to form MgO and $MgNb_2O_{3.67}$. These three components prevented MgH_2 grain growth during heating and thus improved its hydrogen sorption kinetics. Jin *et al.* (2007b) ball milled MgH_2 with 1 mol. % of niobium (V) fluoride (NbF_5) for 15 min. The additive was reported to have melted during the milling period and a liquid-solid reaction between the two combining materials led to the formation of fin-like NbH layers along nanocrystalline MgH_2 grain boundaries. The grain growth of nanocrystalline MgH_2 was subdued by the NbH layers and this sustained the additive's catalytic effect up to 10 de/hydrogenation cycles. Role of F in MgF_2 product (during dehydrogenation reaction) or Mg–H–F solid solution in the de/hydrogenation kinetics of MgH_2, according to the researchers, needed further investigations. Niobium (V) fluoride was confirmed by Luo *et al.* (2008) to have a profound influence on the de/hydrogenation kinetics and storage capacity of MgH_2. The composite which was processed by milling MgH_2 together with 2 mol % NbF_5 for 5 h could absorb 56 wt.% H_2 in in 60 min and within the same period, it could desorb 5 wt.% H_2. Results from XRD and XPS proved that Nb species with varying valence states between 0 and +5 was responsible for the improved kinetic performance of the composite. Further investigations on the active species and influence of F^- in the de/hydrogenation reactions were recommended. Porcu *et al.* (2008) employed transmission electron microscopy (TEM) - based techniques to identify the structure and reaction between MgH_2 and Nb_2O_5. The TEM analysis showed that during milling, Nb_2O_5 broke into fragments and were embedded within MgH_2. The smallest fragments stuck to the MgH_2 grains and got embedded within the grain boundaries. This happened after the grains were welded into larger particles. Heating the two compounds yielded reduction of Nb_2O_5 to Nb_2O and MgO was formed. Inter diffusion of MgO and Nb_2O_5 yielded formation of the mixed oxide- $MgNb_2O_{3.67}$. Bi- metallic Nb-V film catalyst added to MgH_2 was recorded to enhance its cycling stability, even beyond 500 de/hydrogenation cycles without causing sorption kinetics distortions (Tan *et al.* 2012). To achieve this, investigators claimed that the surface catalyst distribution and its stability determined the cyclic stability of MgH_2. Ball milling was employed in doping nanosized amorphous NbH_x nanoparticles into MgH_2 (Zhang *et al.* (2015). The composite absorbed 4 wt.% H_2 at 100 °C while at a higher temperature (300 °C), it absorbed 3.3 wt.% H_2. It was reported that the nanosized amorphous NbH_x acted as charge transfer between Mg^{2+} and H^-, which played a major role in the improved hydrogen storage performance of MgH_2. Hydrogen storage of MgH_2/Nb_2O_5 composite was investigated by Pukazhselvan *et al.* (2016). Two different milling media- zirconia and steel, were used and the system was processed by mechanochemically reacting the combining compounds for 30 h. The product was characterized with Nb - dissolved MgO, which provided a catalytic effect on the hydrogen storage properties of MgH_2. Influence of high energy ball milling (HEBM) with isothermal catalytic synergic behaviour of 10 wt.% Nb_2O_5 and TiF_3 on dehydrogenation of MgH_2 was investigated by Zhang *et al.* (2016). Dehydrogenation temperature of MgH_2/TiF_3 was 341 °C, which was 76 °C lower than as-received MgH_2; addition of Nb_2O_5 to MgH_2 resulted in hydrogen being released at a reduced temperature of 336 °C. A combination of these two catalysts to MgH_2 culminated in 310 °C desorption temperature. The non-isothermal synergetic catalytic effect of TiF_3 and Nb_2O_5 was attributed to electronic exchange reactions with hydrogen molecules, which improved the recombination of hydrogen atoms during dehydrogenation. A two-dimensional $Nb_4C_3T_x$ (Mxene) synthesized via chemical exfoliation has been introduced to MgH_2 (Liu *et al.* 2019). Adding 5 wt.% of the additive to the matrix demonstrated good adsorption kinetics. Multilayer structure with OH- terminations and F terminations were generated on the surface of the additive. NbH_x was formed after ball milling and de/hydrogenation cycles. The NbHx was found to be evenly dispersed in the matrix. Onset temperature for ball milled MgH_2 was approximately 297 °C while that of the composite was recorded as 151 ^{0}C. Within 800 ^{0}C, the composite releases H_2 completely within 800 s. Yahya *et al.* (2018) ball milled 1-20 wt.% K_2NbF_7 with MgH_2 powders. The composite comprising MgH_2/5 wt.% K_2NbF_7 was the most effective as it lowered the dehydrogenation temperature of MgH_2 to 225 °C. This composite absorbed 5.1 wt.% H_2 after 43 s at 320 °C while as-milled could absorb this quantity within 76 s at the same temperature. At lower temperature, the composite absorbed 4.7 wt.% H_2 after 30 min while as-milled MgH_2 could absorb 0.7 wt.% at the same time. The active species that led to the improvement of MgH_2 hydrogen storage properties were KH and Nb that were formed during the process. Hollow spherical o-Nb_2O_5 made of 50 nm wall thickness and mossy surfaces was synthesized and ball milled with MgH_2 for 24 h to improve its hydrogen storage properties (Zhang *et al.* 2020). The composite (MgH_2/7 wt.% o- Nb_2O_5) desorbed 6.4 wt.% H_2 at 195 °C; at room temperature, the dehydrogenated composite began to reabsorb hydrogen, and 5.7 wt.% H_2 was achieved at 150 °C. It was reported that high valence Nb^{+5} state of Nb_2O_5 was gradually lowered to Nb^{+4} and Nb^{+2} and finally Nb^0 during

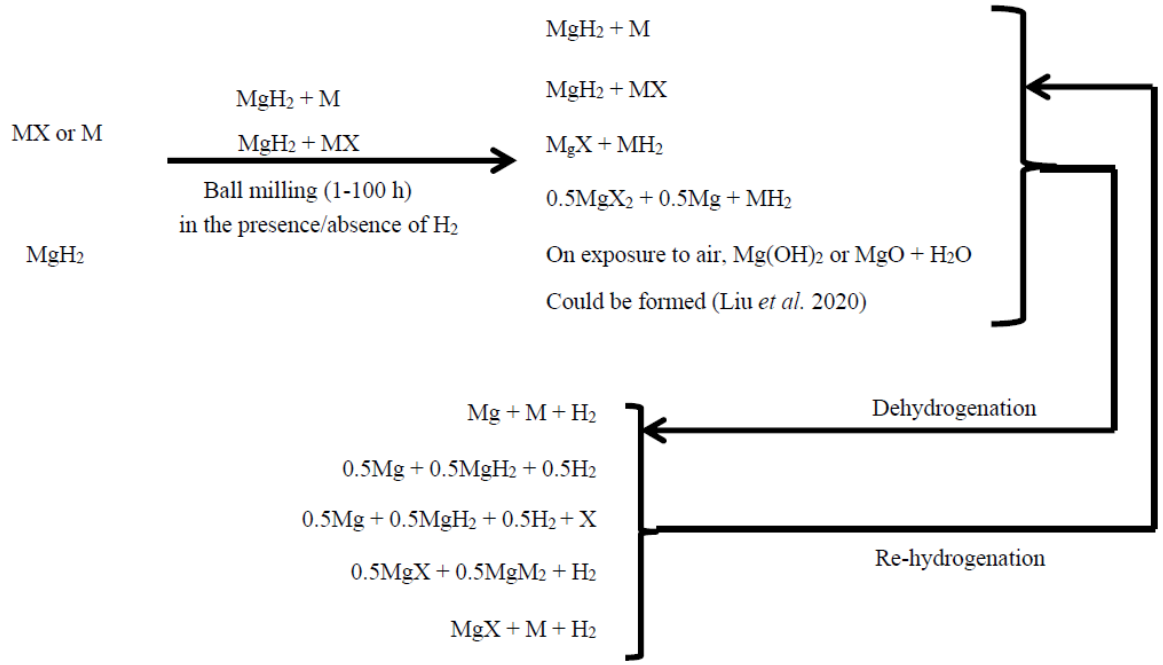

Fig 6. Simple possible reactions involving MgH_2 with transition metals/transition metal-based compounds, M= Transition metal; X = one of H, O, C, S or elements in group VII on the periodic table, N.B. Equation could be complex if M is a transition metal – based alloy or if additives are more than one.

milling followed by first dehydrogenation cycle. It was concluded that the *in situ* formed low-valence Nb acted as de facto catalytic species which lowered the kinetic barriers of MgH_2 hydrogen sorption. This culminated in its decreased dehydrogenation/hydrogenation temperatures Nanoparticles of $V_4Nb_{18}O_{55}$ have been synthesized to aid the catalytic effect of Nb_2O_5 on MgH_2 hydrogen storage properties (Meng *et al.* 2022). Desorption temperature of MgH_2 was reduced to 225 °C; synergistic effect between both V^{5+} and Nb^{5+} improved hydrogen desorption properties of MgH_2. When MgH_2 was doped with 5 wt.% Nb nanocatalyst (prepared via surfactant assisted ball milling technique), stable NbH was formed; this acted as active catalytic unit diminished the energy obstacle and boost MgH_2 kinetics (Nyahuma *et al.* 2022). The composite began to release hydrogen at 186.7 °C, while additive- free s MgH_2 stated hydrogen release at 347 °C. Niobium (V) oxide nanoparticles grafted on MOF (Nb_2O_5@MOF) has been synthesized and doped into MgH_2 (Zhang *et al.* (2023), A slight loss in composite's hydrogen storage capacity was attributed to the formations of MgO and NbO emanating from the reactions between MgH_2 and Nb_2O_5. However, there was a synergetic effect between Nb_2O_5 and MOF which enhanced hydrogen drift between Mg/MgH_2 boundaries; it also prevented Mg/MgH_2 from agglomeration and growth. Ultrafine and steadily dispersed NbC (niobium carbide) nanoparticles enclosed by carbon substrate (NbC/C) was produced via carbon thermal shock method and ball milled with MgH_2 (Jia *et al.* 2023). Particles of MgH_2 were refined by NbC while the substrate (carbon) destabilized Mg-H bond. In addition, multi valence electron transfer existed between positively charged Nb ions and NbH_x (formed *in situ*). In addition, the electron transfer also occurred between Mg and H atoms which influenced Mg/MgH_2 reversible transformation. These were the outcomes of the catalytic influence of NbC/C.

4. Summary and Conclusion

Researches involving the use of Ti, Ni, V, Mo, Fe, Cr, Co, Zr and Nb in their monoatomic forms, alloys (with transition or other metals), intermetallics and composites to better MgH_2 hydrogen storage features have been reviewed. These transition metal-based additives are often doped in MgH_2 via ball milling in the presence or absence of hydrogen. Depending on the milling time and other conditions considered, reaction often occurs during milling which culminates in the formation of new phase(s) (see Figure 6); in situations where combining materials remain unchanged after milling, transformation occurs during de/hydrogenation which engenders the existence of new phase(s). Asides causing uniform distribution of additives throughout MgH_2 matrix, mechanical milling has also been proven to create suitable surface area that acts as catalyst sites. In addition to the prevalence of some monoatomic transition metal after hydrogenation-dehydrogenation cycles, phases such as TiH_2, Mg_2Ni, Mg_2NiH_4, V_2O, VH_2, MoSe, Mg_2FeH_6, NbH and Nb_2O_5 have imparted catalytic effects through creation of diffusion channels for hydrogen by weakening Mg – H bond strength. This reduces hydrogen de/sorption temperatures, remove energy barrier for de/hydrogenation (which results to activation energy reduction) and in turn, hastens MgH_2 hydrogen absorption and desorption kinetics. Grain growth of MgH_2 can also be prevented by the catalysts during heating to improve its hydrogen storage capacity. Transition metals such as Ti, Fe and Nb can exist in multiple valence states and they often aid charge transfer between Mg^+ and H^- to positively influence hydrogen sorption kinetics. It is also observed that the hydrogen storage operation of MgH_2/transition metal –based materials will depend on the kind of additive used (including formulations), MgH_2/additive mixing ratio, ball milling time, ball–to-combining materials ratio and de/hydrogenation cycle

(including temperature and holding time involved). There is need for more investigations to be carried out on nanostructured binary and ternary transition metal – based materials (alloys, intermetallics and or their combinations) as additives to amplify the hydrogen storage properties of MgH_2. In addition, the already established compounds (TiH_2, Mg_2Ni, Mg_2NiH_4, V_2O, VH_2, MoSe, Mg_2FeH_6, NbH, and Nb_2O_5) formed after ball milling or de/hydrogenation can be processed and directly doped into MgH_2.

References

Aceves, S.M., Frias, J.M., & Villazana, G. (2000). Analytical and Experimental Evaluation of Insulated Pressure Vessels for Cryogenic Hydrogen Storage. *International Journal of Hydrogen Energy*, *25*(11), 1075-1085; https://doi.org/10.1016/S0360-3199(00)00016-1

Aceves, S.M., Loza, F.E., Orozco, E.L., Ross, T.O., Weisberg, A.H., Brunner, T.C., & Kircher, O. (2010). High-density Automotive Hydrogen Storage with Cryogenic Capable Pressure Vessels. *International Journal of Hydrogen Energy*, *35*(3), 1219-1226; https://doi.org/10.1016/j.ijhydene.2009.11.069

Al Ghafri, S.Z.S., Swanger, A., Jusko, V., Siahvashi, A., Perez, F., Johns, M.L., & May, E.F. (2022). Modelling of Liquid Hydrogen Boil-Off. *Energies*, *15*(3), 1-16; https://doi.org/10.3390/en15031149

Ali, N.A., Yahya, M.S., Sazelee, N., Din, M.F.M., & Ismail, M. (2022). Influence of Nanosized CoTiO3 Synthesized via a Solid-State Method on the Hydrogen Storage Behavior of MgH2. *Nanomaterials,* *12*(7), 1-18; https://doi.org/10.3390/nano12173043

An, C., Liu, G., Li, L., Wang, Y., Chen, C.C., Wang, Y., Jiao, L., & Yuan, H. (2014). In Situ Synthesized One-Dimensional Porous Ni@C Nanorods as Catalysts for Hydrogen Storage Properties of MgH2. *Nanoscale*, *6*, 3223–3230; 10.1039/C3NR05607D

Assfour, B., Leoni, S., Seifert, G., & Baburin, I.A. (2011). Packings of Carbon Nanotubes – New Materials for Hydrogen Storage. *Advanced Materials*, *23*, 1237–1241; https://doi.org/10.1002/adma.201003669

Barison, S., Agresti, F., Russo, S.L., Maddalena, A., Palade, P., Principi, G., & Torzo, G. (2008). A Study of the $LiNH_2$–MgH_2 System for Solid State Hydrogen Storage. *Journal of Alloys and Compounds*, *459*(1–2), 343-347; https://doi.org/10.1016/j.jallcom.2007.04.278

Baroutaji, A., Arjunan, A., Ramadan, A., Alaswad, A., Achour, H., Abdelkareem, M.A., & Olabi, A.G. (2022). Nanocrystalline Mg_2Ni for Hydrogen Storage. *Encyclopedia of Smart Materials*, *2*, 366-370; https://doi.org/10.1016/B978-0-12-815732-9.00061-9

Bassetti, A., Bonetti, E., Pasquini, L., Montone, A., Grbovic, J., & Antisari, M.V. (2005). Hydrogen Desorption from Ball Milled MgH_2 Catalyzed with Fe. *The European Physical Journal B*, *43*, 19-27; https://doi.org/10.1140/epjb/e2005-00023-9

Baum L., Meyer, L., & Ze´lis, M. (22007). Hydrogen Storage Properties of the Mg/Fe System. *Physica B*, *389*,189–192; https://doi.org/10.1016/j.physb.2006.07.054

Ben, T., Pei, C., Zhang, D., Xu, J., Deng, F., Jing, X., & Qiu, S. (2011). Gas Storage in Porous Aromatic Frameworks (PAFs). *Energy & Environmental Science*, *4*, 3991–3999; https://doi.org/10.1039/C1EE01222C

Berezovets, V.V., Denys, R.V., Zavaliy, I.Y., & Kosarchyn, Y.V. (2022).Effect of Ti-Based Nanosized Additives on the Hydrogen Storage Properties of MgH2. *International Journal of Hydrogen Energy*, *47*(11), 7289-7298; https://doi.org/10.1016/j.ijhydene.2021.03.019

Bhatnagar, A., Johnson, J.K., Shaz, M.A., & Srivastava, O.N. (2018). TiH2 as a Dynamic Additive for Improving the De/Rehydrogenation Properties of MgH2: A Combined Experimental and Theoretical Mechanistic Investigation. *The Journal of Physical Chemistry C*, *122*(37), 21248–21261; https://doi.org/10.1021/acs.jpcc.8b07640

Bhatnagar, A., Pandey, S.K., Vishwakarma, A.K., Singh, S., Shukla, W., Soni, P.K., Shaz, M.A., & Srivastava, O.N. (2016). Fe_3O_4@Graphene as a Superior Catalyst for Hydrogen De/Absorption from/in MgH_2/Mg. *Journal of Materials Chemistry A*, *4*, 14761–14772; https://doi.org/10.1039/c6ta05998h

Cabo, M., Garroni, S., Pellicer, .E., Milanese, C., Girella, A., Marini, A., Rossinyol, E., Suriñach, S., & Baró, M.D. (2011). Hydrogen Sorption Performance of MgH_2 Doped with Mesoporous Nickel- and Cobalt-Based Oxides. *International Journal of Hydrogen Energy*, *36*(9), 5400-5410; https://doi.org/10.1016/j.ijhydene.2011.02.038

Chen, F., Liang, J., Zhao, J., Tao, Z., & Chen, J. (2008). Biomass Waste-Derived Microporous Carbons with Controlled Texture and Enhanced Hydrogen Uptake. *Chemistry of Materials*, *20*(5), 1889–1895; https://doi.org/10.1021/cm702816x

Chen, G., Zhang, Y., Chen, J., Zhu, Y., & Li, L. (2018). Enhancing Hydrogen Storage Performances of MgH_2 by Ni Nano-Particles Over Mesoporous Carbon CMK-3. *Nanotechnology*, *29*, 1-11; https://doi.org/10.1088/1361-6528/aabcf3

Chen, M., Pu, Y., Li, Z., Huang, G., Liu, X., Lu, Y., Tang, W., Xu, L., Liu, S., Yu, R., & Shui1, J. (2020). Synergy between Metallic Components of MoNi Alloy for Catalyzing Highly Efficient Hydrogen Storage of MgH_2. *Nano Research*, 1-7; https://doi.org/10.1007/s12274-020-2808-7

Chen, R., Wang, X., Xu, L., Chen, L., Li, S., & Chen, C. (2010).An Investigation on the Reaction Mechanism of $LiAlH_4$–MgH_2 Hydrogen Storage System. *Materials Chemistry and Physics*, *124*(1), 83-87; https://doi.org/10.1016/j.matchemphys.2010.05.07

Chen, Y., Wu, C.Z., Wang, P., & Cheng, H.M. (2006). Structure and Hydrogen Storage Property of Ball-Milled $LiNH_2$/MgH_2 Mixture. *International Journal of Hydrogen Energy*, *31*(9), 1236-1240; https://doi.org/10.1016/j.ijhydene.2005.09.001

Cheng, C., Zhang, H., Song, M., Wu, F., & Zhang, L. (2023). Research Regarding Molybdenum Flakes' Improvement on the Hydrogen Storage Efficiency of MgH_2. *Metals*, *13*, 1-11; https://doi.org/10.3390/met13030631

Cheng, Y., Bi, J., & Zhang, W. (2021). The Hydrogen Storage Properties of MgH_2–Fe_7S_8 Composites. *Materials Advances*, *2*, 736-742; 10.1039/d0ma00818d

Croston, D.L., Grant, D.M., & Walker, G.S. (2010). The Catalytic Effect of Titanium Oxide Based Additives on the Dehydrogenation and Hydrogenation of Milled MgH_2. *Journal of Alloys and Compounds*, *492*(1–2), 251-258; https://doi.org/10.1016/j.jallcom.2009.10.19

Cui, J., Liu, J., Wang, J., Ouyang, L., Sun, D., Zhu, M. & Yao, X. (2014). Mg–TM (TM: Ti, Nb, V, Co, Mo or Ni) Core–Shell Like Nanostructures: Synthesis, Hydrogen Storage Performance and Catalytic Mechanism. *Journal of Materials Chemistry A*, *2*, 9645–9655; https://doi.org/10.1039/C4TA00221K

Cui, J., Wang,, H., Liu, J., Ouyang, L., Zhang, Q., Sun, D., Yao, X., & Zhu, M. (2013). Remarkable Enhancement in Dehydrogenation of MgH_2 by a Nano-Coating of Multi-Valence Ti-Based Catalysts. *Journal of Materials Chemistry A*, *1*, 5603–5611; https://doi.org/10.1039/C3TA01332D

Da- Conceição, M.O.T., Brum, M.C., & Dos Santos, D.S. (2014). The Effect of V, VCl_3 and VC Catalysts on the MgH_2 Hydrogen Sorption Properties. *Journal of Alloys and Compounds, 586*, S101–S104; https://doi.org/10.1016/j.jallcom.2012.12.131

Dan, L., Hu, L., Wang, H., & Zhu, M. (2019). Excellent Catalysis of MoO_3 on the Hydrogen Sorption of MgH_2. *International Journal of Hydrogen Energy*, *44*(55), 29249-29254; https://doi.org/10.1016/j.ijhydene.2019.01.285

Dehouche, Z., Goyette, J., Bose, T.K., & Schulz, R. (2003). Moisture Effect on Hydrogen Storage Properties of Nanostructured MgH_2–V–Ti Composite. *International Journal of Hydrogen Energy*, *28*,(9), 983-988; https://doi.org/10.1016/S0360-3199(02)00196-9

Dehouche, Z., Klassen, T., Oelerich, W., Goyette, J., Bose, T.K., & Schulz, R. (2002). Cycling and Thermal Stability of Nanostructured MgH_2–Cr_2O_3 Composite for Hydrogen Storage. *Journal of Alloys and Compounds*, *347*(12), 319-323; https://doi.org/10.1016/S0925-8388(02)00784-3

Doğan, M., Sabaz, P., Bïcïl, B., Kizilduman, B.K.K., & Turhan, Y. (2020). Activated Carbon Synthesis from Tangerine Peel and its Use in Hydrogen Storage. *Journal of the Energy Institute*, *95*(6), 2176-2185; https://doi.org/10.1016/j.joei.2020.05.011

Dong, J., Wang, X., Xu, H., Zhao, Q., & Li, J. (2007). Hydrogen Storage in Several Microporous Zeolites. *International Journal of Hydrogen Energy*, *32*, 4998 – 5004; https://doi.org/10.1016/j.ijhydene.2007.08.009

Du, H., Liu, G., Da, Z., & Min, E. (1999). Synthesis, Characterization and Catalytic Properties of VS-2. *Studies in Surface Science and Catalysis, 105*, 741-746; https://doi.org/10.1016/S0167-2991(97)80624-6

Du, X., Ding, Y., Song, F., Ma, B., Zhao, J., & Song, J. (2015). Efficient Photocatalytic Water Oxidation Catalyzed by Polyoxometalate $[Fe_{11}(H_2O)_{14}(OH)_2(W_3O_{10})_2$- $(\alpha$-$SbW_9O_{33})_6]^{27}$- Based on Abundant Metals. *Chemical Communications Journal*, *51*, 13925-13928; 10.1039/c5cc04551g

Edalati, K., Uehiro, R., Ikeda, Y., Li, H.W., Emami, H., Filinchuk, Y., Arita , M., Sauvage, X., Tanaka, I., Akiba, E., & Horita, Z. (2018). Design and Synthesis of a Magnesium Alloy for Room Temperature Hydrogen Storage. *Acta Materiala*, *149*, 88-96; https://doi.org/10.1016/j.actamat.2018.02.033

Edwards, P.P., Kuznetsov, V.I., & David, W.T.F. (2007). Hydrogen Energy. *Philosophical Transactions of the Royal Society A*, *365*, 1043–1056; https://doi.org/10.1098/rsta.2006.1965

El-Eskandarany, M.S., Al-Ajmi, F., Banyan, M., & Al-Duweesh, A. (2019). Synergetic Effect of Reactive Ball Milling and Cold Pressing on Enhancing the Hydrogen Storage Behavior of Nanocomposite MgH_2/10 wt% $TiMn_2$ binary system. *International Journal of Hydrogen Energy*, *44*(48), 6428-26443; https://doi.org/10.1016/j.ijhydene.2019.08.093

Farha, O.K., Yazaydin , A.O., Eryazici, I., Malliakas, C.D., Hauser, B.G., Kanatzidis, M.G., Nguyen, S.T., Snurr, R.Q., & Hupp, J.T. (2010). De Novo Synthesis of a Metal–Organic Framework Material Featuring Ultrahigh Surface Area and Gas Storage Capacities. *Nature Chemistry*, *2*, 944-948; https://doi.org/10.1038/nchem.834

Filiz, B.C. (2021). Investigation of the Reaction Mechanism of the Hydrolysis of MgH_2 in $CoCl_2$ Solutions under Various Kinetic Conditions. *Reaction Kinetics, Mechanisms and Catalysis*, *132*, 93-109; https://doi.org/10.1007/s11144-020-01923-4

Friedrichs, O., Zinsou, F.A., Fernández, J.R.A., Sánchez-López, J.C., Justo, A., Klassen, T., Bormann, R., & Fernández, A. (2006). MgH_2 with Nb_2O_5 as Additive, for Hydrogen Storage: Chemical, Structural and Kinetic Behavior with Heating. *Acta Materialia*, *54*(1), 105-110; https://doi.org/10.1016/j.actamat.2005.08.024

Fu, Y., Ding, Z., Ren, S., Li, X., Zhou, S., Zhang, L., Wang, W., Wu, L., Li, Y., & Han, S. (2020). Effect of In-Situ Formed Mg_2Ni/Mg_2NiH_4 Compounds on Hydrogen Storage Performance of MgH_2. *International Journal of Hydrogen Energy*, *45*(52), 28154-28162; https://doi.org/10.1016/j.ijhydene.2020.03.089

Furukawa, H., Ko, N., Go, Y.B., Aratani, N., Choi, S.B., Choi, E., Yazaydin, A.O., Snurr, R.Q., Keeffe, M.O., Kim, J., & Yaghi, O.M. (2010). Ultrahigh Porosity in Metal-Organic Frameworks. *Science, 329*, 424–428; 10.1126/science.1192160

Gao, H., Liu, Y., Zhu, Y., Zhanhg, J., & Li, L. (2020). Catalytic Effect of Sandwich-Like Ti_3C_2/TiO_2(A)-C on Hydrogen Storage Performance of MgH_2. *Nanotechnology*, *31*, 1-11; https://doi.org/10.1088/1361-6528/ab5979

Gao, H., Shi, R., Zhu, J., Liu, Y., Shao, Y., Zhu, Y., Zhang, J., Li, L., & Hu, X. (2021). Interface Effect in Sandwich Like Ni/Ti_3C_2 Catalysts on Hydrogen Storage Performance of MgH_2. *Applied Surface Science*, *564*, 1-8; https://doi.org/10.1016/j.apsusc.2021.150302

Gao, S., Wang, H., Wang, X., Liu, H., He, T., Wang, Y., Wu, C., Li, S., & Yan, M. (2020). $MoSe_2$ Hollow Nanospheres Decorated with $FeNi_3$ Nanoparticles for Enhancing the Hydrogen Storage Properties of MgH_2. *Journal of Alloys and Compounds*, *830*, 1-12; https://doi.org/10.1016/j.jallcom.2020.154631

Gao, S., Wang, X., Liu, H., He, T., Wang, Y., Li, S., & Yan, M. (2019). Effects of Nano-Composites (FeB, FeB/CNTs) on Hydrogen Storage Properties of MgH_2, *Journal of Power Sources*, *438*, 227006; https://doi.org/10.1016/j.jpowsour.2019.227006

Gao, S., Wang, X., Liu, H., He, T., Wang, Y., Li, S., & Yan, M. (2020). CNTs decorated with CoFeB as a Dopant to Remarkably Improve the Dehydrogenation/Rehydrogenation Performance and Cyclic Stability of MgH_2. *International Journal of Hydrogen Energy*, *45*(53), 28964-28973; https://doi.org/10.1016/j.ijhydene.2020.07.148

Gattia, D.M., Jangir, M., & Jain, I.P. (2019). Study on Nanostructured MgH_2 with Fe and its Oxides for Hydrogen Storage Applications. *Journal of Alloys and Compounds*, *801*,188-191; https://doi.org/10.1016/j.jallcom.2019.06.067

Han, Z., Zhou, S., Chen, H., Nu, H., & Wang, N. (2017). Enhancement of the Hydrogen Storage Properties of Mg/C Nanocomposites Prepared by Reactive Milling with Molybdenum. *Journal of Wuhan University of Technology-Materials Science Edition*, 299-304; 10.1007/s11595-017-1596-8

Han, Z., Zhou, S., Wang, N., Zhang, Q., Zhang, T., & Ran, W. (2016). Crystal Structure and Hydrogen Storage Behaviors of Mg/MoS_2 Composites from Ball Milling. *Journal of Wuhan University of Technology-Materials Science Edition*, 773-778; 10.1007/s11595-016-1444-2

Hanada, N., Ichikawa, T., & Fujii, H. (2005). Catalytic Effect of Ni nano-Particle and Nb Oxide on H-Desorption Properties in MgH_2 Prepared by Ball Milling. *Journal of Alloys and Compounds*, *404–406*, 716-719; https://doi.org/10.1016/j.jallcom.2004.12.166

Hao, S., & Sholl, D.S. (2012). Effect of TiH_2 - Induced Strain on Thermodynamics of Hydrogen Release from MgH_2. *The Journal of Physical Chemistry C*, *116*, 2045-2050; dx.doi.org/10.1021/jp210573a

Hirscher, M. & Panella, B. (2007). Hydrogen Storage in Metal–Organic Frameworks. *Scripta Materialia*, *56*, 809-812; https://doi.org/10.1016/j.scriptamat.2007.01.005

Hong, F., Fu, H., Shi, W., Zhao, R., Li, R., Fan, Y., Liu, Z., Ding, S., Liu, H., Zhou, W., Guo, J., & Lan, Z. (2023). Application of Nitrogen-Doped Graphene-Supported Titanium Monoxide as a Highly Active Catalytic Precursor to Improve the Hydrogen Storage Properties of MgH_2. *Journal of Alloys and Compounds*, *960*, 1-10; https://doi.org/10.1016/j.jallcom.2023.170727

Hou, Q., Yang, X., & Zhang, J.(2021). Review on Hydrogen Storage Performance of MgH_2; Development and Trends. *Chemistry Europe*, 1589-1606; https://doi.org/10.1002/slct.202004476

Hu, C., Zheng, Z., Si, T., & Zhang, Q. (2022). Enhanced Hydrogen Desorption Kinetics and Cycle Durability of Amorphous $TiMgVNi_3$-doped MgH_2. *International* Journal *of Hydrogen Energy*, *7*(6,), 3918-3926; https://doi.org/10.1016/j.ijhydene.2021.11.010

Huang, T., Huang, X., Hu, C., Wang, J., Liu, H., Ma, Z., Zou, J., & Ding, W. (2021). Enhancing Hydrogen Storage Properties of MgH_2 through Addition of $Ni/CoMoO_4$ Nanorods. *Materialstoday Energy*, *19*, 1-11; https://doi.org/10.1016/j.mtener.2020.100613

Huang, Z., Xia, K., Zheng, L., Han, B., Gao, Q., Wang, H., Li, Z., & Zhou, Z. (2017). Facile and Scalable Synthesis of Hierarchically Porous Graphene Architecture for Hydrogen Storage and High-Rate Supercapacitors. *Journal of Materials Science: Materials in Electronics*, *28*, 17675-17681; https://doi.org/10.1007/s10854-017-7705-9

Huot, J., Pelletier, J.F., Lurio, L.B., Sutton, M., & Schulz, R. (2003). Investigation of Dehydrogenation Mechanism of MgH_2–Nb Nanocomposites. *Journal of Alloys and Compounds*, *348*(1-2), 319-324; https://doi.org/10.1016/S0925-8388(02)00839-3

Ismail, M., Zhao, Y., Xuebin, Y., & Dou, S.X. (2012). Improved Hydrogen Storage Performance of MgH_2 $NaAlH_4$ Composite by Addition of TiF_3. *International Journal of Hydrogen Energy*, *37*(10), 8395-8401; https://doi.org/10.1016/j.ijhydene.2012.02.117

Ismail, M., Zhao, Y., Xuebin, Y., Mao, J.F., & Dou, S.F. (2011). The Hydrogen Storage Properties and Reaction Mechanism of the MgH_2–$NaAlH_4$ Composite System. *International Journal of Hydrogen Energy*, *36*(15), 9045-9050; https://doi.org/10.1016/j.ijhydene.2011.04.132

Jia, Y., Han, S., Zhang, W., Zhao, X., Sun, P., Liu, Y., Shi, H., & Wang, J. (2013). Hydrogen Absorption and Desorption Kinetics of MgH_2 Catalyzed by MoS_2 and MoO_2. *International Journal of Hydrogen Energy*, *38*(5), 2352-2356; https://doi.org/10.1016/j.ijhydene.2012.12.018

Jia, Y., Wang, X., Hu, L., Xiao, X., Zhang, S., He, J., Qi, J., Lv, L., Xu, F., Sun, L., & Chen, L. (2023). Carbon Composite Support Improving Catalytic Effect of NbC Manoparticles on the Low-Temperature Hydrogen Storage Performance of MgH_2. *Journal of Materials Science & Technology*, *150*, 65-74; https://doi.org/10.1016/j.jmst.2022.11.044

Jiang, W., Wang, H., & Zhu, M. (2021). AlH_3 as a Hydrogen Storage Material: Recent Advances, Prospects and Challenges. *Rare Metals*, *40*, 3337–3356; https://doi.org/10.1007/s12598-021-01769-2

Jiang, Y., Yu, Y., Wang, Z., Zhang, S., & Cao, J. (2023), CFD Simulation of Heat Transfer and Phase Change Characteristics of the Cryogenic Liquid Hydrogen Tank under Microgravity Conditions. *International, Journal of Hydrogen Energy*, *48*(19), 7026-7037; https://doi.org/10.1016/j.ijhydene.2022.04.006

Jin, S.A., Shim, J.H., Ahn, J.P., Cho, Y.W., & Yi, K.W. (2007b). Improvement in Hydrogen Sorption Kinetics of MgH_2 with Nb Hydride Catalyst. *Acta Materialia*, *55*(15), 5073-5079; https://doi.org/10.1016/j.actamat.2007.05.029

Jin, S.A., Shim, J.H., Cho, Y.W., & Yi, K.W. (2007a). Dehydrogenation and Hydrogenation Characteristics of MgH_2 with Transition Metal Fluorides. *Journal of Power Sources*, *172* (2), 25,859-862; https://doi.org/10.1016/j.jpowsour.2007.04.090

Kadri, A., Jia, Y., Chen, Z., & Yao, X. (2015). Catalytically Enhanced Hydrogen Sorption in Mg-MgH_2 by Coupling Vanadium-Based Catalyst and Carbon Nanotubes. *Materials*, *8*, 3491-3507; https://doi.org/10.3390/ma8063491

Konstas, K., Taylor, J.W., Thornton, A.W., Doherty, C.M., Lim, W.X., Bastow, T.J., Kennedy, D.F., Wood, C.D., Cox, B.J., Hill, J.M., Hill, A.J., & Hill, M.R. (2012). Lithiated Porous Aromatic Frameworks with Exceptional Gas Storage Capacity. *Angewandte Chemie International Edition*, *51*, 6639 –6642; https://doi.org/10.1002/ange.201201381

Krainz, G., Bartlok, G., Bodner, P., Casapicola, P., Doeller, C., Hofmeister, F., Neubacher, E., & Zieger, A. (2004), Development of Automotive Liquid Hydrogen Storage Systems. Advances in Cryogenic Engineering. *Transactions of the Cryogenic Engineering Conference-CEC*, *49*, 35-40; https://doi.org/10.1063/1.1774664

Krishna, R., Titus, E., Salimian, M., Okhay, O., Rajendran, S., Rajkumar, A., Sousa, J.M.G., Ferreira, A.L.C., Gil, J.C., & Gracio, J. (2012). Hydrogen Storage for Energy Application. *INTECH*, 243-266; https://doi.org/10.5772/51238

Kumar, S., Jain, A., Yamaguchi, S., Miyaoka, H., Ichikawa, T., Mukherjee, A., Dey, G.K., & Kojima, Y. (2017). Surface Modification of MgH_2 by $ZrCl_4$ to Tailor the Reversible Hydrogen Storage Performance. *International Journal of Hydrogen Energy*, *42*(9), 6152-6159; https://doi.org/10.1016/j.ijhydene.2017.01.193

Kumar, S., Singh, P.K., Rao, G.v.S.N., Kojima, Y., & Kain, V. (2018). Synergic Effect of Vanadium Trichloride on the Reversible Hydrogen Storage Performance of the Mg-MgH_2 System. *International Journal of Hydrogen Energy*, *43*(32), 15330-15337; https://doi.org/10.1016/j.ijhydene.2018.06.063

Lan, J., Cao, D., Wang, D., Ben, T., & Zhu, G.(2010). High-Capacity Hydrogen Storage in Porous Aromatic Frameworks with Diamond-Like Structure. *Physical Chemistry Letters*, *1*, 978–981; https://doi.org/10.1021/jz900475b

Lan, Z., Wen, X., Zeng, L., Luo, Z., Liang, H., Shi, W., Hong, F., Liu, H., Ning, H., Zhou, W., & Guo, J. (2022). In Situ Incorporation of Highly Dispersed Nickel and Vanadium Trioxide Nanoparticles in Nanoporous Carbon for the Hydrogen Storage Performance Enhancement of Magnesium Hydride. *Chemical Engineering Journal*, *446*(3), 1-12; https://doi.org/10.1016/j.cej.2022.137261

Langmi, H.W., Book, D., Walton, A., Johnson, S.R., Al-Mamouri, M.M., Speight, J.D., Edwards, P.P., Harris, I.R., & Anderson, P.A. (2005). Hydrogen Storage in Ion - Exchanged Zeolites. *Journal of Alloys and Compounds*, *404–406*, 637–642; https://doi.org/10.1016/j.jallcom.2004.12.193

Li, L., Jiang, G., Tian, H., & Wang, Y. (2017). Effect of the Hierarchical Co@C Nanoflowers on the Hydrogen Storage Properties of MgH_2. *International Journal of Hydrogen Energy*, *42*(47), 28464-28472; https://doi.org/10.1016/j.ijhydene.2017.09.160

Li, P., Wan, Q., Li, Z., Zhai, F., Li, Y., Cui, L., Qu, X., & Qu, A.A. (2013). MgH_2 Dehydrogenation Properties Improved by $MnFe_2O_4$ Nanoparticles. *Journal of Power Sources*, *239*, 201-206; https://doi.org/10.1016/j.jpowsour.2013.03.096

Li, X., Fu, Y., Xue, Y., Cong, L., Yu, H., Zhang, L. Li, Y., & Han, S. (2021). Effect of Ni/tubular g-C_3N_4 on Hydrogen Storage Properties of MgH_2. *International Energy of Hydrogen Energy*, *46*, 33186 - 33196; https://doi.org/10.1016/j.ijhydene.2021.07.166

Li, Y., Hu, F., Luo, L., Xu, J., Zhao, Z., Zhang, Y., & Zhao, D. (2018). Hydrogen Storage of Casting MgTiNi Alloys. *Catalysis Today*, *318*, 103-106; https://doi.org/10.1016/j.cattod.2017.10.046

Liang, G., Huo, J., Boily, S., Neste, A.V., & Schulz, R. (1999). Hydrogen Storage Properties of the Mechanically Milled MgH –V_2 Nanocomposite. *Journal of Alloys and Compounds*, *291*, 295–299; https://doi.org/10.1016/S0925-8388(99)00268-6

Liang, G., Huot, J., Boily, S., Neste, V., & Schulz, R. (2000). Hydrogen Storage in Mechanically Milled Mg–$LaNi_5$ and MgH_2 –$LaNi_5$ Composites. *Journal of Alloys and Compounds*, *297*, 261–265; https://doi.org/10.1016/S0925-8388(99)00592-7

Liu, G., Wang, L., Hu, Y., Sun, C., Leng, H., Li, Q., & Wu, C. (2021). Enhanced Catalytic Effect of TiO_2@rGO Synthesized by One-Pot Ethylene Glycol-Assisted Solvothermal Method for MgH_2. *Journal of Alloy and Compounds*, *881*, 1-10; https://doi.org/10.1016/j.jallcom.2021.160644

Liu, H., Lu, C., Wang, X., Xu, Li., Huang,, X., Wang,, X. & Ning, H. (2021). Combinations of V_2C and Ti_3C_2 MXenes for Boosting the Hydrogen Storage Performances of MgH_2. *ACS Applied Materials & Interfaces*, 13235−13247; https://doi.org/10.1021/acsami.0c23150

Liu, H., Sun, P., Bowman Jr., R.C., Fang, Z.Z., Liu, Y., & Zhou, C. (2020). Effects of Air Exposure on Hydrogen Storage Properties of Catalyzed Magnesium Hydride. *Journal of Power Sources*, *454*, 1-10; https://doi.org/10.1016/j.jpowsour.2020.227936

Liu, X., Zhang, C., Geng, Z., & Cai, M. (2014). High-Pressure Hydrogen Storage and Optimizing Fabrication of Corncob-Derived Activated Carbon. *Microporous and Mesoporous Materials*, *194*, 60-65; https://doi.org/10.1016/j.micromeso.2014.04.005

Liu, Y., Gao, H., Zhu, Y., Li, S., Zhang, J., & Li, L. (2019). Excellent catalytic Activity of a Two-Dimensional $Nb_4C_3T_x$ (MXene) on Hydrogen Storage of MgH_2. *Applied Surface Science*, *493*, 431-440; https://doi.org/10.1016/j.apsusc.2019.07.037

Lu, C., Liu, H., Xu, L., Luo, H., He, S., Duan, X., Huang, X., Wang, X., Lan, Z., & Guo, J. (2022). Two-Dimensional Vanadium Carbide for Simultaneously Tailoring the Hydrogen Sorption Thermodynamics and Kinetics of Magnesium Hydride. *Journal of Magnesium and Alloys*, *10*(4),1051-1065; https://doi.org/10.1016/j.jma.2021.03.030

Lu, J., Cho, Y.J., Fang, Z.Z., Sohn, H.Y., & Ro¨nnebro, E. (2009). Hydrogen Storage Properties of Nanosized MgH_2-0.1TiH_2 Prepared by Ultrahigh-Energy-High-Pressure Milling. *Journal of the American Chemical Society*, *131*, 15843–15852; https://doi.org/10.1021/ja906340u

Lu, X., Zhang, L., Zheng, J., & Yu, X. (2022). Construction of Carbon Eovered Mg_2NiH_4 Nanocrystalline for Hydrogen Storage. *Journal of Alloys and Compounds*, *905*, 1-11; https://doi.org/10.1016/j.jallcom.2022.164169

Lu, Y., Wang, H., Liu, J., Liuzhang, O., & Zhu, M. (2018). Destabilizing the Dehydriding Thermodynamics of MgH_2 by Reversible Intermetallics Formation in Mg−Ag−Zn Ternary Alloys. *Journal of Power Sources*, *396* (31); 796-802; https://doi.org/10.1016/j.jpowsour.2018.06.060

Lu, Z., He, J., Song, M., Zhang, Y., Wu, F., Zheng, J., Zhang, L., & Chen, L. (2023). Bullet like Vanadium-Based MOFs as a Highly Active Catalyst for Promoting the Hydrogen Storage Property in MgH_2. *International Journal of Minerals, Metallurgy and Material*, *30*(1), 44-53; https://doi.org/10.1007/s12613-021-2372-5

Luo, W. (2004). ($LiNH_2$–MgH_2): A Viable Hydrogen Storage System. *Journal of Alloys and Compounds*, *381*(1–2), 284-287; https://doi.org/10.1016/j.jallcom.2004.03.119

Luo, Y., Wang, P., Ma, L.P., & Cheng, H.M. (2008). Hydrogen Sorption Kinetics of MgH_2 Catalyzed with NbF_5. *Journal of Alloys and Compounds*, *453*(1-2), 138-142; https://doi.org/10.1016/j.jallcom.2006.11.113

Ma, Z., Zhang, J., Zhu, Y., Lin, H., Lin, Y., Zhang, Y., Zhu, D., & Li, L. (2018). Facile Synthesis of Carbon Supported Nano-Ni Particles with Superior Catalytic Effect on Hydrogen Storage Kinetics of MgH_2. *ACS Applied Energy Materials*, *1*, 1158−1165; https://doi.org/10.1021/acsaem.7b00266

Ma, Z., Zou, J., Khan, D., Zhu, W., Hu, C., Zeng, X., & Ding, W. (2019). Preparation and Hydrogen Storage Properties of MgH_2-Trimesic Acid-TM MOF (TM=Co, Fe) Composites. *Journal of Materials Science & Technology*, *35*(10), 2132-2143; https://doi.org/10.1016/j.jmst.2019.05.04

Madina, V., & Azkarate, T. (2009), Compatibility of Materials with Hydrogen. Particular Case: Hydrogen Embrittlement of Titanium Alloys. *International Journal of Hydrogen Energy*, *34*(14), 976-5980; https://doi.org/10.1016/j.ijhydene.2009.01.058

Malahayati, Nurmalita, Ismail, Machmud, M.N., & Jalil, Z. (2021). Sorption Behavior of MgH_2-Ti for Hydrogen Storage Material Prepared by High Pressure Milling. *Journal of Physics: Conference Series*, *1882*, 1-5; 10.1088/1742-6596/1882/1/012005

Malka, I.E., Bystrzycki, J., Plocinski, T., & Czujko, T. (2011). Microstructure and Hydrogen Storage Capacity of Magnesium Hydride with Zirconium and Niobium Fluoride Additives after Cyclic Loading. *Journal of Alloys and Compounds*, *509*, S616-S620; https://doi.org/10.1016/j.jallcom.2010.10.122

Mao, J., Guo, Z., Yu, X., Liu, H., Wu, Z., & Ni, J. (2010). Enhanced Hydrogen Sorption Properties of Ni and Co-Catalyzed MgH_2. *International Journal of Hydrogen Energy*, *35*(10), 4569-4575; https://doi.org/10.1016/j.ijhydene.2010.02.107

Meng, Y., Ju, S., Chen, W., Chen, X., Xia, G., Sun, D., & Yu, X. (2022). Design of Bifunctional Nb/V Interfaces for Improving Reversible Hydrogen Storage Performance of MgH_2. *Small Structures, 3*, 1-10; 10.1002/sstr.202200119

Muthukumar P., Prakash, M.M., & Murthy, S.S. (2005). Experiments on a Metal Hydride Based Hydrogen Storage Device. *International Journal of Hydrogen Energy*, *30*, 1569-1581; https://doi.org/10.1016/j.ijhydene.2004.12.007

Nathaniel, L.R., Juergen, E., Mohamed, E., David, T.V.O., Keeffe, M., Kim, J., & Yaghi, O.M. (2003). Hydrogen Storage in Microporous Metal–Organic Frameworks. *Science, 300*, 1127–1129; 10.1126/science.1083440

Nishihara, H., Hou, P.X., Li, L.X., Ito, M., Uchiyama, M., Kaburagi, T., Ikura, A., Katamura, J., Kawarada, T., Mizuuchi, K., & Kyotani, T. (2009). High-pressure Hydrogen Storage in Zeolite-Templated Carbon. *The Journal of Physical Chemistry C*, *113*, 3189–3196; https://doi.org/10.1021/jp808890x

Nyahuma, F.M., Zhang, L., Song, M., Lu, X., Xiao, B., Zheng, J., & Wu, F. (2022). Significantly Improved Hydrogen Storage Behaviors in MgH_2 wit h Nb Nanocatalyst. International *Journal of Minerals, Metallurgy and Materials*, *29*(9), 1789-1797; https://doi.org/10.1007/s12613-021-2303-5

Oladunni, O.J., Mpofu, K., & Olanrewaju, O.A. (2022). Greenhouse Gas Emissions and its Driving Forces in the Transport Sector of South Africa. *Energy Reports*, *8*, 2052-2061; https://doi.org/10.1016/j.egyr.2022.01.123

Olubusoye, O.E., & Musa, D. (2020). Carbon Emissions and Economic Growth in Africa: Are they Related? *Cogent Economics & Science*, *8*, 1-21; https://doi.org/10.1080/23322039.2020.1850400

Patelli, N., Calizz, M., Migliori, A., Morandi, V., & Pasquini, L. (2017). Hydrogen Desorption Below 150 °C in MgH_2−TiH_2 Composite Nanoparticles: Equilibrium and Kinetic Properties. *The Journal of Physical Chemistry C*, *121*, 11166−11177; https://doi.org/10.1021/acs.jpcc.7b03169

Polanski, M., Bystrzycki, J., Varin, R.A., Plocinski , T., & Pisarek, M. (2011). The Effect of Chromium (III) Oxide (Cr_2O_3) Nanopowder on the Microstructure and Cyclic Hydrogen Storage Behavior of Magnesium Hydride (MgH_2). *Journal of Alloys and Compounds*, *509*(5), 2386-2391; https://doi.org/10.1016/j.jallcom.2010.11.026

Porcu, M., Long, A.K.P., & Sykes, J.M. (2008). TEM Studies of Nb_2O_5 Catalyst in Ball-Milled MgH_2 for Hydrogen Storage. *Journal of Alloys and Compounds*, *453*(1-2), 341-346; https://doi.org/10.1016/j.jallcom.2006.11.147

Prabhukhot, P.R. Wagh, M.M., & Gangal, A.C. (2016). A Review on Solid State Hydrogen Storage Material. *Advances in Energy and Power*, *4*(2), 11–22; https://doi.org/10.13189/aep.2016.040202

Pukazhselvan, D., Irurueta ,G.O., Pérez, J., Singh, B., Bdikin, I., Singh, M.J.K., & Fagg, D. P. (2016). Crystal Structure, Phase Stoichiometry and Chemical Environment of $Mg_xNb_yO_{x+y}$ Nanoparticles and their Impact on Hydrogen storage in MgH_2. *International Journal of Hydrogen Energy*, *41*(27), 11709-11715; https://doi.org/10.1016/j.ijhydene.2016.04.029

Pukazhselvan, D., Nasani, N., Correia, P., Argibay, E.C., rurueta, G.O., Stroppa, D.G., & Fagg, D.B. (2017a). Evolution of Reduced Ti Containing Phase(s) in MgH_2/TiO_2 System and its Effect on the Hydrogen Storage Behavior of MgH_2. *Journal of Power Sources*, *362*, 174-183; https://doi.org/10.1016/j.jpowsour.2017.07.032

Pukazhselvan, D., Nasani, N., Sandhya, K.S., Singh, B., Bdikin, I., Koga, N., & Fagg, D.P. (2017b). Role of Chemical Interaction between MgH_2 and TiO_2 Additive on the Hydrogen Storage Behavior of MgH_2. *Applied Surface Science*, *420*, 740-745; https://doi.org/10.1016/j.apsusc.2017.05.182

Pukazhselvan, D., Sandhya, K.S., Ramasamy, D., Shaula, A., & Fagg, D.P. (2020). Transformation of Metallic Ti to TiH_2 Phase in the Ti/MgH_2 Composite and Its Influence on the Hydrogen Storage Behavior of MgH_2. *ChemPhysChem*, *21*, 1-8; https://doi.org/10.1002/cphc.202000031

Pukazhselvan, D., Silva, D.A.R., Sandhya, K.S., Fateixa, S.F., Shaula, A., Nogueira, H., Bdikin, I., & Fagg, D.P. (2022). Interaction of Zirconia with Magnesium Hydride and its Influence on the Hydrogen Storage Behavior of Magnesium Hydride. *International Journal of Hydrogen Energy*, *47*(51), 21760-21771; https://doi.org/10.1016/j.ijhydene.2022.04.290

Qiu, Y., Yang, H., Tong, L., & Wang, L. (2021). Research Progress for Cryogenic Materials for Storage and Transportation of Liquid Hydrogen. *Metals, 11*(1101), 1-13; https://doi.org/10.3390/met11071101

Rahwanto, A., Ismail, I., Nurmalita, N., Mustanir,, & Jalil1, Z. (2021). Nanoscale Ni as a Catalyst in MgH_2 for Hydrogen Storage Material. *Journal of Physics: Conference Series*, *1882*, 1-5; doi:10.1088/1742-6596/1882/1/012010

Ranjbar, A., Guo, Z.P., Yu, X.B., Attard, D., Calka, A., & Liu, H.K. (2009b). Effects of SiC Nanoparticles with and without Ni on the Hydrogen Storage Properties of MgH_2. *International Journal of Hydrogen Energy*, *34*(17), 7263-7268; https://doi.org/10.1016/j.ijhydene.2009.07.005

Ranjbar, A., Guo, Z.P., Yu, X.B., Wexler, D., Calka, A., Kim, C.J., & Liu, H.K. (2009a). Hydrogen Storage Properties of MgH_2–SiC Composites. *Materials Chemistry and Physics*, *114*(1), 168-172; https://doi.org/10.1016/j.matchemphys.2008.09.001

Ren, L., Zhu, W., Li, Y., Lin, X., Xu, H., Sun, F., Lu, C., & Zou, J. (2022). Oxygen Vacancy-Rich 2D TiO_2 Nanosheets: A Bridge Toward High Stability and Rapid Hydrogen Storage Kinetics of Nano-Confned MgH_2. *Nano-Micro Letters*, *14*(114), 1-16; https://doi.org/10.1007/s40820-022-00891-9

Rivoirard, S., De Rango, P., Fruchart, D., Charbonnier, J., & Vempaire, D. (2003). Catalytic Effect of Additives on the Hydrogen Absorption Properties of Nano-Crystalline MgH_2(X) Composites. *Journal of Alloys and Compounds 356–357*, 622–625; https://doi.org/10.1016/S0925-8388(03)00145-2

Ródena, N.A.L., Guo, Z.X., Zinsou, K.F.A. Amorós, D.C., & Solano, A.L. (2008). Effects of Different Carbon Materials on MgH_2 Decomposition, *Carbon*, *46*(1), 126-137; https://doi.org/10.1016/j.carbon.2007.10.033

Rosi, N.L., Eckert, J., Eddaoudi, M., Vodak, D.T., Kim, J., Keeffe, M.O., & Yaghi, O.M. (2003). Hydrogen Storage in Microporous Metal-Organic Frameworks. *Science*, *300*, 1127- 1129; https://doi.org/10.1126/science.1083440

Santos, S.F., Ishikawa, T.T., Botta, W.J., & Huot, J. (2014). MgH_2 + FeNb Nanocomposites for Hydrogen Storage. *Materials Chemistry and Physics*, *147*(3), 557-562; https://doi.org/10.1016/j.matchemphys.2014.05.031

Sazelee, N.A., Idris, N.H., Din, M.F.D., Mustafa, N.S., Ali, N.A., Yahya, M.S., Yap, F.A.H., Sulaiman, N.I.N., & Israel, M. (2018). Synthesis of $BaFe_{12}O_{19}$ by Solid State Method and its Effect on Hydrogen Storage Properties of MgH_2. *International Journal of Hydrogen Energy*, *43*(45), 20853-20860; https://doi.org/10.1016/j.ijhydene.2018.09.125

Schimmel, H.G., Huot, H., Chapon, L.C., Tichelaa, F.D., & Mulder, F.M. (2005). Hydrogen Cycling of Niobium and Vanadium Catalyzed Nanostructured Magnesium. *Journal of the American Chemical Society*, *127*, 14348-14354; https://doi.org/10.1021/ja051508a

Sethia, G., & Sayar, A. (2016). Activated Carbon with Optimum Pore Size Distribution for Hydrogen Storage. *Carbon*, *99*, 289 – 294; https://doi.org/10.1016/j.carbon.2015.12.032

Setijadi, E.J., Li, X., Masters, A.F., Maschmeyer, T., & Zinsou, K.F.A. (2016).Delaminated MoS_2 as a Structural and Functional Modifier for MgH_2 – Better Hydrogen Desorption Kinetics through Induced Worm-Like Morphologies. *International Journal of Hydrogen Energy*, *41*(5), 3551-3560; https://doi.org/10.1016/j.ijhydene.2015.12.161

Shahi, R.R., Bhatanagar, A., Pandey, S.K., Shukla, V., Yadav, T.P., Shaz, M.A., & Srivastava, O.N. (2015). MgH_2-$ZrFe_2H_x$ Nanocomposites for Improved Hydrogen Storage Characteristics of MgH_2. *International Journal of Hydrogen Energy*, *40*(35), 11506-11513; https://doi.org/10.1016/j.ijhydene.2015.03.162

Shan, J., Li, P., Wan, Q., Zhai, F., Zhang, J., Li, Z., Liu, Z., Volinsky, A.A., & Qu, X. (2014). Significantly improved dehydrogenation of Ball-Milled MgH_2 Doped with $CoFe_2O_4$ Nanoparticles. *Journal of Power*

Sources, *268*, 778-786; https://doi.org/10.1016/j.jpowsour.2014.06.116

Shao, H., Felderhoff, M., & Schüth, F. (2011). Hydrogen Storage Properties of Nanostructured MgH_2/TiH_2 Composite Prepared by Ball Milling Under High Hydrogen Pressure. *International Journal of Hydrogen Energy*, *36*(17), 10828-10833; https://doi.org/10.1016/j.ijhydene.2011.05.180

Shao, H., Huang, Y., Guo, H., Liu, Y., Guo, Y., & Wang, Y. (2021). Thermally Stable Ni MOF Catalyzed MgH_2 for Hydrogen Storage. *International Journal of Hydrogen Energy*, *46*(76), 37977-37985; https://doi.org/10.1016/j.ijhydene.2021.09.045

Shao, Y., Gao, H., Tang, Q., Liu, Y., Liu, J., Zhu, Y., Zhang, J., Li, L., Hu, X., & Ba, Z. (2022). Ultra-fine TiO_2 Nanoparticles Supported on Three-Dimensionally Ordered Nacroporous Structure for Improving the Hydrogen Storage Performance of MgH_2. *Applied Surface Science*, *585*, 1-10; https://doi.org/10.1016/j.apsusc.2022.152561

Shigemura, M., Lecuona, E., & Sznajder, J.I. (2017). Effects of Hypercapnia on the Lung. *The Journal of Physiology*, *595*(8), 2431–2437; https://doi.org/10.1113/JP273781

Singh, G., Bahadur, .R., Lee, M., Kim, I.Y., Ruban, A.M., Davidraj, J.M., Semit, D., Karakoti, A., Al Muhtaseb, A.H., & Al Vinu, A. (2021). Nanoporous Activated Biocarbons with High Surface Areas from Alligator Weed and their Excellent Performance for CO_2 Capture at both Low and High Pressures. *Chemical Engineering Journal*, *406*, 1-11; https://doi.org/10.1016/j.cej.2020.126787

Song, M., Zhang, L., Yao, Z., Zheng,, J., Shang,, D., Chen, L. & Li, H. (2022). Unraveling the Degradation Mechanism for the Hydrogen Storage Property of Fe Nanocatalyst-Modified MgH_2. *Inorganic Chemistry Frontiers*, *9*, 3874–3884; https://doi.org/10.1039/d2qi00863g

Soni, P.K., Bhatnagar, A., & Shaz, M.A. (2023). Enhanced Hydrogen Properties of MgH_2 by Fe Nanoparticles Loaded Hollow Carbon Spheres. *International Journal of Hydrogen Energy*, *48*(47), 17970-17982; https://doi.org/10.1016/j.ijhydene.2023.01.278

Stephen, F.L. (2005), Fossil Fuels in the 21st Century, *Ambio*, *34*(8), 621–627; https://www.jstor.org/stable/4315666

Taghizadeh-hesary, F., Rasoulinezhad, E., Yoshino, N., Chang, Y., Taghizadeh-hesary, F., & Morgan, P. (2021). The Energy–Pollution–Health Nexus: A Panel Data Analysis of Low- and Middle-Income Asian Countries. *The Singapore Economic Review*, *66*(2), 435-455; https://doi.org/10.1142/S0217590820430043

Takeichi, N., Senoh, H., Yokota, T., Tsuruta, H., Tsuruta, H., Hamada, K., Takeshita, H.T., Tanaka, H., Kiyobayashi, T., Takano, T., & Kuriyama, N.(2003). Hybrid Hydrogen Storage Vessel, a Novel High-Pressure Hydrogen Storage Vessel Combined with Hydrogen Storage Material. *International Journal of Hydrogen Energy*, *2*(10), 1121-1129; https://doi.org/10.1016/S0360-3199(02)00216-1

Tian, G., Wu, F., Zhang, H., Wei, J., Zhao, H., & Zhang, L. (2023). Boosting the Hydrogen Storage Performance of MgH_2 by Vanadium Based Complex Oxides. *Journal of Physics and Chemistry of Solids*, *174*, 1-9; https://doi.org/10.1016/j.jpcs.2022.111187

Tan, M., & Shang, C. (2012). Effect of TiC and Mo_2C on Hydrogen Desorption of Mechanically Milled MgH_2. *Journal of Chemical Science and Technology*, *1*(2), 54-59.

Tan, X.H., Zahiri, B., Holt, C.M.B., Kubis, A., & Mitlin, D. (2010). A TEM Based Study of the Microstructure During Room Temperature and Low Temperature Hydrogen Storage Cycling in MgH_2 Promoted by Nb–V. *Acta Materialia*, *60*(16), 5646-5661; https://doi.org/10.1016/j.actamat.2012.06.009

Thongtan, P., Dansirima, P., Thiangviriya, S., Thaweelap, N., Plerdsranoy, P., & Utke, R. (2018). Reversible Hydrogen Sorption and Kinetics of Hydrogen Storage Tank Based on MgH_2 modified by TiF_4 and Activated carbon. *International Journal of Hydrogen*, *22*, 12260-12270; https://doi.org/10.1016/j.ijhydene.2018.04.171

Ud-Din, R., Xuanhui, Q., Zahid, G.H., Asghar, Z., Shahzad, M., Iqbal, M., & Ahmad, E. (2014). Improved Hydrogen Storage Performances of MgH_2–$NaAlH_4$ System Catalyzed by TiO_2 Nanoparticles. *Journal of Alloys and Compounds*, *604*(15), 317-324; https://doi.org/10.1016/j.jallcom.2014.03.150

United States Environmental Protection Agency. https://www.epa.gov/ghgemissions/overview-greenhouse-gases (Cited May 20, 2023).

Van der Werf, G.R., Morton, D.C., DeFries, R.S., Olivier, J.G., Kasibhatla, P.S., Jacson, R.B., Collatz, G.J., & Randerson, J.T. (2009) CO_2 Emissions from Forest Loss, *Nature Gesccience*, *2*, 737-738; https://doi.org/10.1038/ngeo671

Verma, S.K., Shaz, M.A., & Yadav, T.P. (2023). Enhanced Hydrogen Absorption and Desorption Properties of MgH_2 with Graphene and Vanadium Disulfide. *International Journal of Hydrogen Energy*, *48*(56), 21383-21394; https://doi.org/10.1016/j.ijhydene.2021.12.269

Wang, A., Ren,, Z., Jian, N., Gao, M., Hu, J., Du, F., Pan, H., & Liu, Y. (2018). Vanadium Oxide nanoparticles Supported on Cubic Carbon Nanoboxes as Highly Active Catalyst Precursors for Hydrogen Storage in MgH_2. *Journal of Materials Chemistry A*, *6*, 16177–16185; https://doi.org/10.1039/C8TA05437A

Wang, H., Geo, Q., & Hu, J. (2009). High Hydrogen Storage Capacity of Porous Carbons Prepared by using Activated Carbon, *Journal of the American Chemical Society*, *131*, 7016–7022; https://doi.org/10.1021/ja8083225

Wrobel-Iwaniec, I., Díez, N., & Gryglewicz, G. (2015), Chitosan-Based Highly Activated Carbons for Hydrogen Storage. *International Journal of Hydrogen Energy*, *40*(17), 5788-5796; https://doi.org/10.1016/j.ijhydene.2015.03.034

Wronski, Z.S., Carpenter, G.J.C., Czujko, T., & Varin, R.A. (2011). A New Nanonickel Catalyst for Hydrogen Storage in Solid-State Magnesium Hydrides. *International Journal of Hydrogen Energy*, *36*(1), 1159-1166; https://doi.org/10.1016/j.ijhydene.2010.06.089

Xu, G., Shen, N., Chen, L., Chen, Y., & Zhang, W. (2017). Effect of $BiVO_4$ Additive on the Hydrogen Storage Properties of MgH_2. *Materials Research Bulletin*, *89*, 197-203; https://doi.org/10.1016/j.materresbull.2017.01.036

Yang, J., Cai, W., Ma, M., Li, L., Liu, C., Ma, X., Li, L., & Chen, X. (2020). Driving Forces for China's CO_2 Emissions from Energy Consumption Based on Kanya-LMDI Methods. *Science of The Total Environment*, *711*, 1-15; https://doi.org/10.1016/j.scitotenv.2019.134569

Yang, Z., Xia, Y., & Mokaya, Y. (2007). Enhanced Hydrogen Storage Capacity of High Surface Area Zeolite-Like Carbon Materials. *Journal American Chemical Society*, *129*, 1673-1679; https://doi.org/10.1021/ja067149g

Yanya, M.S., & Ismail, M. (2018). Synergistic Catalytic Effect of $SrTiO_3$ and Ni on the Hydrogen Storage Properties of MgH_2. *International Journal of Hydrogen Energy*, *43*(12), 6244-6255; https://doi.org/10.1016/j.ijhydene.2018.02.028

Yahya, M.S., Sulaiman, N.N., Mustafa, N.S., Yap, F.A.H., & Ismail, M. (2018). Improvement of Hydrogen Storage Properties in MgH_2 Catalysed by K_2NbF_7. *International Journal of Hydrogen Energy*, *43*(31), 14532-14540; https://doi.org/10.1016/j.ijhydene.2018.05.157

Yao, G., Jiang, Y., Liu, Y., Wu, C., Chao, K.C., Lyu, C., & Li, Q. (2020). Catalytic Effect of Ni@rGO on the Hydrogen Storage Properties of MgH_2. *Journal of Magnesium and Alloys*, *8*, 461-471; https://doi.org/10.1016/j.jma.2019.06.006

Yavari, A.R., LeMoulec, A., De- Castro, F.R., Deledda, S., Friedrichs, O., Botta, W.J., Vaughan, V.G., Klassen, T., Fernandez, A., & Kvick, A. (2005). Improvement in H-Sorption Kinetics of MgH_2 Powders by Using Fe *Nanoparticles* Generated by Reactive FeF_3 Addition. *Scripta Materialia*, *52*(8), 719-724. https://doi.org/10.1016/j.scriptamat.2004.12.020

Yu, T.C., Lin, C.C., Chen, C.C., Lee, W.L., Lee, R.G., Tseng, G.H., & Liu, S.P.(2013). Wireless Sensor Networks for Indoor Air Quality Monitoring. *Medical Engineering & Physics*, *35*(2), 231-235; https://doi.org/10.1016/j.medengphy.2011.10.011

Yu, X., Yang, Z.X., Liu, H.K., Grant, D.M., & Walker, G.S. (2010). The Effect of a Ti-V-based BCC Alloy as a Catalyst on the Hydrogen Storage Properties of MgH_2. *International Journal of Hydrogen Energy*, *35*(12), 6338-6344; https://doi.org/10.1016/j.ijhydene.2010.03.089

Yu, Z., Zhang, W., Zhang, Y., Fu, Y., Cheng, Y., Guo, S., Li, Y. & Han, S. (2023). Remarkable Kinetics of Novel Ni@CeO_2–MgH_2 Hydrogen Storage Composite. *International Journal of Hydrogen Energy*, *47*(83), 35352-35364; https://doi.org/10.1016/j.ijhydene.2022.08.121

Yuan, W., Li, B., & Li, L. (2011). A Green Synthetic Approach to Graphene Nanosheets for Hydrogen Adsorption. *Applied Surface*

Science, *257*, 10183-10187; https://doi.org/10.1016/j.apsusc.2011.07.015

Zahiri,, B., Danaie, M., Tan, X., Amirkhiz, B.S., Botton, C.A., & Mitlin, D. (2011). Stable Hydrogen Storage Cycling in Magnesium Hydride, in the Range of Room Temperature to 300 ºC, Achieved Using a New Bimetallic Cr-V Nanoscale Catalyst. *The Journal of Physical Chemistry C*, *116*, 3188–3199; https://.doi.org/10.1021/jp211254k

Zaluski, L., Zaluska, A., & Olsen, J.O.S .(1995a). Hydrogen Absorption in Manocrystalline Mg_2Ni Formed by Mechanical Alloying. *Journal of Alloys and Compounds*, *217*(2), 245-249; https://doi.org/10.1016/0925-8388(94)01348-9

Zaluski, L., Zaluska, A., Tessier, P., Olsen, J.O.S., & Schulz, R. (1995b). Catalytic Effect of Pd on Hydrogen Absorption in Mechanically Alloyed Mg_2Ni, $LaNi_5$ and FeTi. *Journal of Alloys and Compounds*, *217*(2), 295-300; https://doi.org/10.1016/0925-8388(94)01358-6

Zhang, F., Zhao, P., Niu, M., & Maddy, J. (2016).The Survey of Key Technologies in Hydrogen Energy Storage. *International Journal of Hydrogen Energy*, *41*(33), 14535–14552; https://doi.org/10.1016/j.ijhydene.2016.05.293

Zhang, J., He, L., Yao, Y., Zhou, X.J., Yu, L.P., & Zhou, D.W. (2020). Catalytic Effect and Mechanism of NiCu Solid Solutions on Hydrogen Storage Properties of MgH_2. *Renewable Energy*, *154*, 1229-1239; https://doi.org/10.1016/j.renene.2020.03.089

Zhang, J., Hou, Q., Guo, X., & Yang, X. (2022c). Achieve High-Efficiency Hydrogen Storage of MgH_2 Catalyzed by Nanosheets $CoMoO_4$ and rGO. *Journal of Alloys and Compound*s, *911*, 1-13; https://doi.org/10.1016/j.jallcom.2022.165153

Zhang, J., Li, L., Chen, R., Xu, P., & Kai, F. (2008). High Pressure Steel Storage Vessels Used in Hydrogen Refueling Station, *Journal of Pressure Vessel Technology*, *130*, 1-3; https://doi.org/10.1115/1.2826453

Zheng, J., Liu, X., Xu, P., Liu, P., Zhao, Y., & Yang, J. (2012). Development of High Pressure Gaseous Hydrogen Storage Technologies. *International Journal of Hydrogen Energy*, *37*(1), 1048–1057; https://doi.org/10.1016/j.ijhydene.2011.02.125

Zhang, L., Ji, L., Yao, Z., Yan, N., Sun, Z., Yang, X., Zhu, X., Hu, S. & Chen, L. (2019). Facile synthesized Fe Nanosheets as Superior Active Catalyst for Hydrogen Storage in MgH_2. *International Journal of Hydrogen Energy*, *44*(39), 21955-21964; https://doi.org/10.1016/j.ijhydene.2019.06.065

Zhang, L., Nyahuma, F.M., Zhang, H., Cheng, C., Zheng, J., Wu, F., & Chen, L. (2023). Metal Organic Framework Supported Niobium Pentoxide Nanoparticles with Exceptional Catalytic Effect on Hydrogen Storage Behavior of MgH_2. *Green Energy & Environment*, *88*(2), 589-600; https://doi.org/10.1016/j.gee.2021.09.004

Zhang, L., Xia, X., Xu, C., Zheng, J., Fan, X., Shao, J., Li, S., Ge, H., Wang, Q., & Chen, L. (2015). Remarkably Improved Hydrogen Storage Performance of MgH_2 Catalyzed by Multivalence NbH_x Nanoparticles. The *Journal of Physical Chemistry C*, *119*, 8554−8562; https://doi.org/10.1021/acs.jpcc.5b01532

Zhang, L., Yu, H., Lu, Z., Zhao, C., Zheng, J., Wei, T., Wu, F., & Xiao, B. (2022b). The Effect of Different Co Phase Structure (FCC/HCP) on the Catalytic Action towards the Hydrogen Storage Performance of MgH_2. *Chinese Journal of Chemical Engineering*, *43*, 343-352; https://doi.org/10.1016/j.cjche.2021.10.016

Zhang, T., Hou, X., Hu, R., Kou, H., & Li, J. (2016). Non-isothermal Synergetic Catalytic Effect of TiF_3 and Nb_2O_5 on Dehydrogenation High-Energy Ball Milled MgH_2. *Materials Chemistry and Physics*, *183*, 65-75; https://doi.org/10.1016/j.matchemphys.2016.08.002

Zhang, W., Xu, G., Cheng, Y., Chen, L., Huo, Q., & Liu, S. (2018). Improved Hydrogen Storage Properties of MgH_2 by the Addition of FeS_2 Micro-spheres. *Dalton Transactions*, *47*, 5217–5225; https://doi.org/10.1039/c7dt04665k

Zhang, X., Wang, K., Zhang, X., Hu, J., Gao, M., Pan1, H., & Liu, Y. (2020). Synthesis Process and Catalytic Activity of Nb_2O_5 Hollow Spheres for Reversible Hydrogen Storage of MgH_2. *International Journal of Energy Research*, 3129-3141; https://doi.org/10.1002/er.6006

Zhang, Y., Tian, Q.F., Liu, S.S., & Sun, L.X. (2008).The Destabilization Mechanism and De/re-hydrogenation Kinetics of MgH_2–$LiAlH_4$ Hydrogen Storage System. *Journal of Power Sources*, *185*(2), 1514-1518; https://doi.org/10.1016/j.jpowsour.2008.09.054

Zhang, Y., Zheng. J., Lu, Z., Song, M., He, J., Wu, F., & Zhang, L. (2022a). Boosting the Hydrogen Storage Performance of Magnesium Hydride with Metal Organic Framework-Derived Cobalt@Nickel Oxide Bimetallic Catalyst. *Chinese Journal of Chemical Engineering*, *52*, 161-171; https://doi.org/10.1016/j.cjche.2022.06.026

Zhao, Y., Zhu, Y., Liu, J., Ma, Z., Zhang, J., Liu, Y., Li, Y., & Li, L. (2021). Enhancing Hydrogen Storage Properties of MgH_2 by Core-Shell CoNi@C. *Journal of Alloys and Compounds*, *862*, 1-8; https://doi.org/10.1016/j.jallcom.2020.158004

Zidan, R. (2010). Aluminum Hydride (Alane). Handbook of Hydrogen Storage: New Materials for Future Energy Storage. *Wiley-VCH Verlag GmbH & Co. KgaA Chapter 9*, 249-277.